NTNU
Norwegian University of
Science and Technology

Optimal Control of Floating Offshore Wind Turbines

Eivind Lindeberg

Master of Science in Engineering Cybernetics
Submission date: June 2009
Supervisor: Thor Inge Fossen, ITK
Co-supervisor: Kjetil Uhlen, Sintef Energiforskning

Norwegian University of Science and Technology
Department of Engineering Cybernetics

Problem Description

The purpose of the thesis is to develop a dynamic simulator that integrates aerodynamics, mechanics and control in a single dynamic model.

The following elements must be considered:

1. Literature study on wind turbines. Give a presentation of different models and methods of analysis found in the literature. Identify the main problems from a control point of view, construction as well as implementation aspects.
2. Derive a dynamic model for an offshore wind turbine. The floating structure should be an anchored cylinder with diameter 10m and draft 100m. The cylinder should be modeled in WAMIT and simulated in 6 DOF using force RAOs. The model should also include models of the wind turbine with blade vibrations.
3. Derive a model-based optimal controller able of handling constraints. Investigate problems due to resonances. Focus should be placed on reducing mechanical loads.
4. Simulate the system in the time-domain and present results for energy/power absorption. The system must be simulated for varying wind loads.
5. Present your findings and theoretical results in the report.

Assignment given: 12. January 2009
Supervisor: Thor Inge Fossen, ITK

Abstract

Floating Offshore Wind Power is an emerging and promising technology that is particularly interesting from a Norwegian point of view because of our long and windy coast. There are however still several remaining challenges with this technology and one of them is a possible stability problem due to positive feedback from tilt motion of the turbine tower.

The focus of this report is to develop a simulator for a floating offshore wind turbine that includes individual, vibrating blades. Several controllers are developed, aiming to use the blade pitch angle and the generator power to control the turbine speed and output power, while at the same time limit the low-frequent motions of the tower and the high-frequent motions of the turbine blades. The prime effort is placed on developing a solution using Model Predictive Control(MPC).

It is not possible to conclude from the simulation results that the designed controllers are able to reduce the blade vibrations. Thus, no great progress has been made on the issue of blade vibrations.

However, the MPC controller works very well for the entire operating range of the turbine. A "fuzzy"-inspired switching algorithm is developed and this handles the transitions between the different operating ranges of the turbine excellently. The problem of positive feedback from the tower motion is handled well, and the simulations do not indicate that this issue should jeopardize the viability of floating offshore wind turbines.

Preface

This report is written for the Wind Turbine Department of Sintef Energy Research and the Department of Engineering Cybernetics at The Norwegian University of Science and Technology (NTNU) in Trondheim from January until June 2009. This thesis is the final part of the Master's degree in Engineering Cybernetics.

I got interested in the area of offshore wind energy as a Summer Intern at Sintef the summer of 2008, and it has been rewarding to work on what I believe is a topic for the future. I hope I can be able to work with wind power and/or power generation also in my professional career.

Delivering this thesis marks the finishing line for five eventful years as a student in Trondheim. At this point I would like to express my gratitude to the Student Society, UKA and ISFiT for making Trondheim Norway's best place to be a student, and for giving me the experience and confidence I need to enter the professional world.

I would like to thank the entire wind energy group at Sintef, and especially Kjetil Uhlen for introducing me to the world of wind power and for always having an open door. I would also like to thank my supervisor Thor Inge Fossen at the Department of Engineering Cybernetics of NTNU for concise feedback.

Deserved thanks go to my office mates, Lars Andreas Wennersberg, Terje Kvangardsnes, Morten Pedersen and Tore Brekke for interesting conversations and useful hints on report writing in Latex. Also, the proofreading help from my brother Lars and my sister Anne has been very helpful. At last, I would like to thank Ane Simensen for highly appreciated support, nurturing and nutrition.

Eivind Lindeberg
June 2009

Contents

List of Figures

List of Tables

Chapter 1

Introduction

1.1 Background

Wind turbines have been used to generate electricity since around the 1960's, and the interest for the field is stronger than ever. The field is rapidly and continuously evolving, a fact that can be illustrated by the growth of the maximum size of commercial wind turbines with 10 000% the last 30 years ($\sim 50kW \rightarrow \sim 5MW$) (Manwell et al. (2002)). The growing awareness of the threat of climate change caused by CO_2 emissions has brought wind energy to the top of the global political agenda, and wind energy is projected to play an important role in the increased production of renewable energy in Norway, Europe and the rest of the world. The European Union plans to increase the total share of renewables in the energy consumption to 20% by 2020, and wind energy's share of the total Europeean electricity production from 7.3% in 2007 to 12-14% by 2020 (EWEA (2008)). Moreover, the Norwegian government has stated a goal to triple the production of wind power to 3 TWh by 2010(*St.meld nr.34* (2006-2007)). The total Norwegian production of wind energy in 2008 was around 1 TWh, and it is currently not expected that Norway will meet the 2010 production goal (NVE (2009)).

For continued growth in European wind energy up to, and beyond 2020, offshore installations are seen as vital. Offshore wind farms enjoy several advantages over their onshore counterparts, such as stronger, more stable winds, a smaller visual and audible impact on the environment, and access to the vast open areas at sea. Several offshore wind farms are already in production, and some of the largest green energy projects in Europe are offshore wind projects. Current offshore wind turbines are mounted to the sea-bed and require rather shallow waters (<40m). Shallow waters are not abundant along Norway's long and windy coast, and thus *floating offshore wind turbines* (FOWT) are very interesting from a Norwegian point of view. FOWT's describes any wind turbine mounted on an anchored floating platform.

FOWT is a new technology. StatoilHydro's Hywind project (StatoilHydro (2009)) is the first full-scale installation and a pilot is being installed in the summer of 2009. Sway, another Norwegian company, plans to follow in 2010. Standard wind turbines are mounted on pillars that are standing on the ground or at the sea bottom. Modern wind turbines are placed up to 100m above ground or sea level, and at deep waters this leads to very high tower constructions - accelerating both installation cost and complexity. By allowing the turbines to float, water depth is no longer a constraint and vast areas at sea are made available for wind power production.

FOWT is still a young technology and several different technical solutions are proposed. Which of these technologies - if any - that will prove to be the most

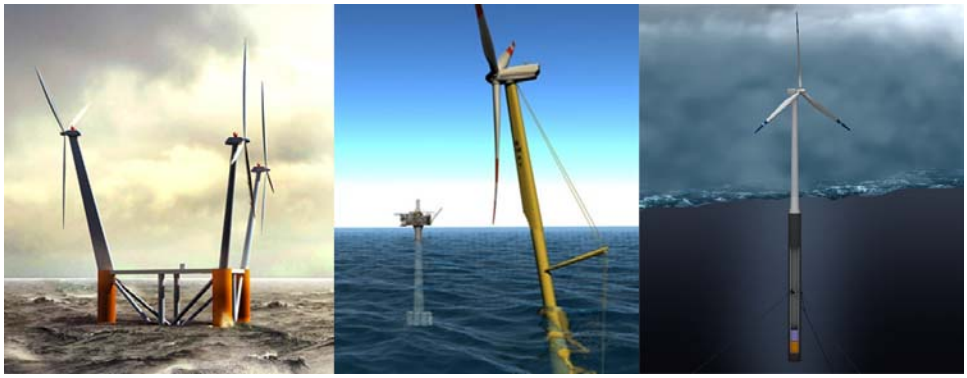

Figure 1.1: Illustration of the three Norwegian FOWT solutions. From left: WindSea, Sway, Hywind

viable is still an open question. Three Norwegian concepts are launched and illustrations of these can be seen in Figure 1.1; WindSea (*Windsea.no* (2008)) is a floating platform with three wind turbines in each corner of a equal-sided triangle. Sway (*sway.no* (2008)) is a single turbine mounted down-wind on an upright pillar, and Hywind is a traditional up-wind wind turbine tower mounted on a deep slender floating structure. A wind turbine is heavy and most of the weight is placed in the nacelle - the top construction of the turbine. To have sufficient stability for the overall floating structure this requires that the platform has a very low center of gravity, which again makes it very heavy. Thus, reducing the top weight of the wind turbine is a crucial task to make floating offshore wind turbines a successful technology.

The increasing size of the wind turbines leads to new challenges as well. Rotor blades over 60 meters long, made to be as light as possible, should still last the lifetime of the turbine. A structure this large will oscillate, so will the tower structure. Vibrations reduces the fatigue life of the turbine, and the expected lifetime of the turbine is an all-important factor for the economical viability of these large scale installations. Designing wind turbine parts in novel, lighter and stronger materials is important, but in addition it is possible to increase the fatigue life of the turbine by designing an intellingent control strategy.

1.2 Literature Survey

Offshore wind technology and the modeling and control of the turbines are now in a period of extensive research. The companies that plan to manufacture them perform their own analysis, and some of this is published. Skaare et al. (2007), Knauer et al. (2006) and Nielsen et al. (2006) give insight into the process and research leading up to StatoilHydro's Hywind project and describe some of the main challenges they have met. StatoilHydro has worked with researchers from among other institutions, Sintef, IFE and NTNU in the process. Two patents have been published proposing two different strategies to reduce oscillations in the structure due to negative damping: Nielsen et al. (2008) and the recently published Skaare (2009)(May, 2009). A third solution to this problem is shown in Larsen & Hanson (2007). These issues will be covered in detail in later chapters.

Extensive research is also carried out outside of the commercial companies. The Norwegian government has in 2009 decided to fund two research centers for Offshore Wind Energy as part of their initiative to start eight so-called *Centres for Environment-Friendly Research*(*St.meld nr.34* (2006-2007)). The centers are The

Norwegian Centre for Offshore Wind Energy (NORCOWE) in Bergen and Norwegian Research Centre for Offshore Wind Technology (NOWITECH) in Trondheim.

Significant research is performed in Denmark by for example the Risø National Laboratory for Sustainable Energy. An example is the overview of the current Offshore Wind Power status presented in Lemming et al. (2007). An investigation of various solutions for floating offshore wind turbines performed by several Dutch scientist is presented in Bulder et al. (2002). The American institution National Renewable Energy Laboratory (NREL) is active in the field. Butterfield et al. (2007) reviews some of the engineering challenges for FOWTs and Wayman et al. (2006) presents a Coupled Dynamic Model of the turbine. NREL has also defined a standard *5MW reference wind turbine for offshore system development* (Jonkman et al. (2009)) to be used by researchers, to make results from different research projects comparable.

Offshore wind energy is also the subject of several PHDs at NTNU at the moment and Fuglseth & Undeland (2007) might be the most relevant one for this thesis.

Fatigue control of blades are another area of intensive research driven by the increasing size and complexity of the wind turbine installations. Kallesøe (2006) presents a method for analyzing blade fatigue and Bossanyi (2003) suggests that individual pitch control (IPC) could be a possibility for reducing blade fatigue loads. Several master thesises on load reduction and IPC have been released; E.g: Selvam (2007) that uses IPC and a *robust control*-strategy for load reduction; Larsen & Mogensen (2006) separates the problem in a collective pitch controller for power and turbine speed regulation, and an individual pitch controller for load reduction; Quirante (2007) uses the same separation approach but implements the power regulation control by means of Model Predictive Control(MPC).

Wind turbine modeling in general is a subject that is covered by several textbooks. Eggleston & Stoddard (1987), Hau (2006), and Manwell et al. (2002) provide an overview of the field, while Munteanu et al. (2008) and Bianchi et al. (2007) are more directed towards simulation and control modeling. Spong et al. (2006) gives thorough insight in rotational matrices and the like, while Fossen (2009) covers the modeling of the floating structure. Several books provides material on control theory: Balchen et al. (2003) and Chen (1999) covers the basics, Skogestad & Postletwaite (2005) deals with multivariable control and Slotine & Li (1991) is a classic within nonlinear control. MPC is the topic of Maciejowski (2002) and van den Boom & Backx (2007).

1.3 Scope of the Report

The goal of this thesis is to develop a controller for a floating offshore wind turbine, that maximizes power output, controls the turbine speed and damps out movements of the floating tower in the pitch direction, parallel to the wind direction. Also, it aims to reduce blade vibrations particularly in the in-plane direction. The control is effectuated by adjusting the (individual) pitch angle of the rotor blades, and the output power of the generator.

The main controller will be developed using Model Predictive Control, and two other controllers will be implemented for comparison. One LQ controller and one slightly modified PID controller.

A simulator for the floating tower, wind turbine and blade dynamics will be implemented in Simulink and Matlab and simulations are performed to assess the performance of the system.

1.4 Organization of the Report

Chapter 2 will go through some basic elements of wind turbine control, and give the reader a brief understanding of existing simple control methods. This chapter aims to introduce any reader not familiar with wind turbines to the topic.

Chapter 3 includes the modeling of the turbine and the floating tower. A non-linear model used for simulation is designed as well as a linearized and simplified model for control purposes.

Chapter 4 describes the development of controllers for the turbine. It aims to provide sufficient theory on the Model Predictive Control method, and the implementation of this controller. Also, some other controllers are introduced showing two patented solutions from the industry.

Chapter 5 shows a range of simulation results to assess the performance of the controllers, and the impact of some of the different parameters in the control design.

Chapter 6 contains the Discussion where the results and findings from the previous chapters are evaluated. This chapter also includes some suggestions for further work in the area.

Chapter 7 is the Conclusion were the main accomplishments are presented, and the final evaluation of the report is made.

Chapter 2

Wind Turbine Fundamentals

2.1 Introduction to Wind Power Production

Wind power production is the science of transforming the energy in moving air - wind - to mechanical, and subsequently, electrical energy. The power that can be extracted from wind is given by the often-seen equation (see e.g. Hau (2006))

$$P_w = \frac{1}{2} A \, \rho \, Cp \, v^3 \tag{2.1}$$

where $A = 2\pi R$ is the total area swept by the turbine blades, R is the length of the blades, ρ is the density of air, v is the wind speed and Cp is the efficiency factor. This efficiency depends on the angle-of-attack between the blades and the relative wind speed. This is adjustable by changing either the rotational speed of the turbine, ω_t, or change the twist angle of the blades, hereafter called the blade pitch angle. The Cp value is bounded above by the so-called Betz limit (Munteanu et al. (2008),p.19), named after German researcher Albert Betz. The Betz limit is found to be 0.59, and describes the theoretical maximum for how much of the kinetic energy in wind that can be transformed to mechanical energy in an ideal wind turbine. Actual wind turbines can achieve maximum efficiencies of between 0.45 and 0.5(Hau (2006)).

The efficiency factor is dependent on both the pitch angle and the so-called tip speed ratio, λ, witch is the ratio between the wind speed and the speed of the blade tip.

$$\lambda = \frac{\omega_t R}{v} \tag{2.2}$$

By adjusting the pitch angle or the rotational speed of the turbine one can control the efficiency of the wind turbine to either maximize produced power or, in strong winds, limit the torque from wind to avoid overloading the generator. The relation between the efficiency factor and the pitch angle or the tip speed ratio respectively, can be seen in Figure 2.1 (a) and (b).

The most popular wind turbine design today is a horizontal axis, three-bladed wind turbine, and this is the design that will be discussed in this thesis.

2.2 Traditional Wind Turbine Control

This section will give a brief, not at all complete, introduction to traditional wind turbine control systems for on-shore installations. The most important difference between on- and offshore installations is that the vibration frequencies of the tower

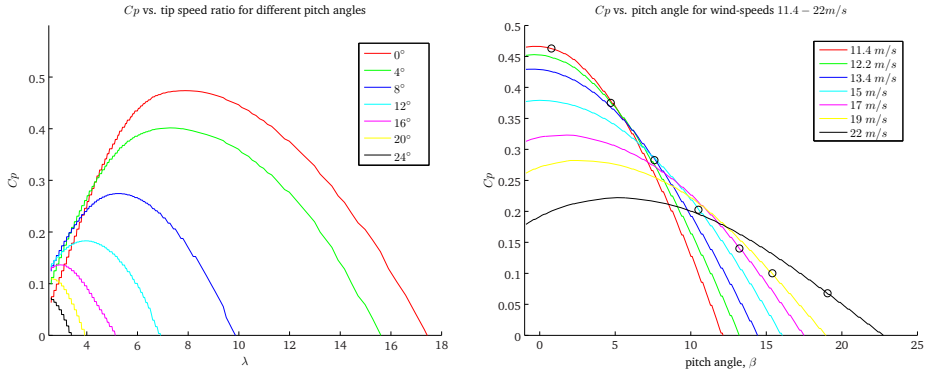

(a) Cp factor for varying tip speed ratio for different pitch angles

(b) Cp factor for varying pitch angle for different wind speeds. $'o'$ indicates the points where the output power is 1

Figure 2.1: Cp-values for varying tip speed ratio (a), and pitch angle (b)

structure for on-shore installations are very high, and outside of the frequenvy band of the pitch controller. This is, however, not the case with floating offshore installations that have very low frequent tower oscillations (MarinTek (2007)). The main objective for an onshore wind turbine controller is to limit incoming torque from strong winds and, for variable speed turbines to ensure that the turbine operates under close to optimal conditions at lower wind speeds.

2.2.1 Fixed Speed Wind Turbines

In the early days of modern wind turbine design the generator in the turbine was directly connected to the power grid, and this implied that the turbine had to rotate at a fixed speed at all times. For this type of turbines pitch control is mostly used to prevent overloading at high wind speed. In order to absorb wind gust this control is fast. Simple PI controllers are widely used, often combined with various gain-scheduling techniques. Other control techniques are also used and Munteanu et al. (2008) suggest e.g. Feedback Linearization, LQ-control, Sliding Mode control(see also Beltran et al. (2008)) as well as robust control strategies.

2.2.2 Variable Speed Wind Turbines

Modern wind turbines, particularly large ones, are usually *variable speed wind turbines*. Variable speed wind turbines have two main advantages; They can adjust the turbine speed to maintain an optimal tip speed ratio, and they can allow the turbine speed to vary slightly to obtain a smoother power output. The desired output power values and turbine speeds for varying wind are presented in Figure 2.2.

From Figure 2.1(a) it can be seen that for zero pitch angle (I.e. at low and medium wind speeds) the optimal tip speed ratio is around 7.5. Thus the goal of the control system should be to maintain this ratio at all times. For strong winds this would imply very high rotation speeds, so this is only valid up to a maximum, or rated, turbine speed. Figure 2.3 shows a block diagram of a typical variable speed wind turbine control system.

The Power setpoint calculation block in Figure 2.3 is the part of the system that implements the variable speed functionality. It decides the output power, based on the current turbine speed.

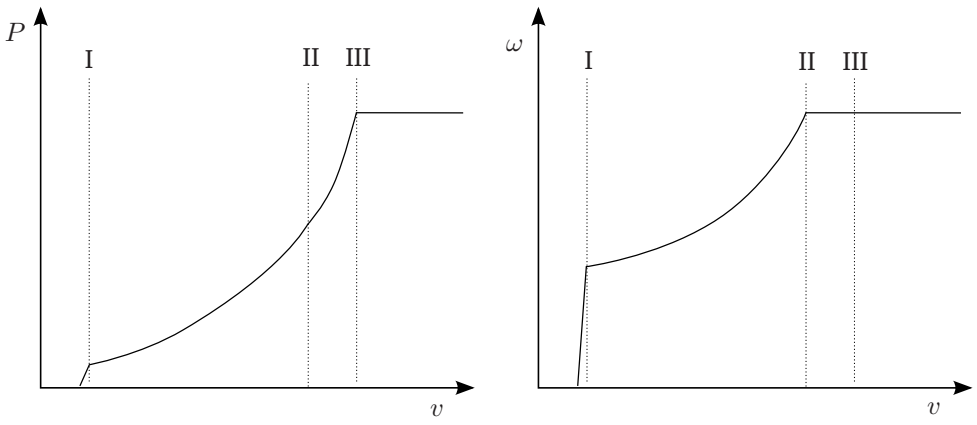

Figure 2.2: Output power(left) and turbine speed(right) for varying wind speed for a typical variable speed wind turbine. I-II is the power maximization area, $\lambda = \lambda_{max}$. II-III is the constant turbine speed area. Over III is the power limitation area

The turbine speed should be adjusted so that the tip-speed ratio is at its optimum at all times. That is:

$$\frac{\omega_t R}{v} = \lambda_{opt} \tag{2.3}$$

This is obtained by keeping the output power at the optimal value for the current turbine speed. By rewriting (2.3)

$$v = \frac{\omega_t R}{\lambda_{opt}} \tag{2.4}$$

an expression for the optimal output power can be obtained:

$$P_{opt} = \frac{1}{2} A \rho C p(\lambda_{opt}, \beta_0) \left(\frac{\omega_t R}{\lambda_{opt}} \right)^3 \tag{2.5}$$

$$P_{opt} = K_{P_{opt}} \omega_t^3 \tag{2.6}$$

This strategy will ensure that the turbine speed will reach the optimum. When the turbine speed is close to its rated value the output power increases. If it increases further the turbine enters the power limitation mode and the output power set-point is kept at the rated value. In order to allow the turbine speed to vary slightly without letting the output power drop below the maximum this constant power area is extended below the rated turbine speed. The size of this area depends on how good the turbine speed controller is. If the turbine speed control is good, the constant power area below rated turbine speed can be small, but if the controller give large oscillations in the rotational speed it has to be larger. A large constant power area reduces the maximum wind speed of the optimization area (I-II in Figure 2.2). The relationship between turbine speed and output power can be seen in Figure 2.4.

2.2.3 Stall Control

In this report the pitch control strategy is to use so-called *pitch-to-feather* control, that is to rotate the blades, using sailing terminology, *out off the wind*. An alternative to this is to use *pitch-to-stall* control which is control by adjusting the blades the other way, i.e. *into the wind*. This will force the blades of the turbine into stall and reduce the torque. Stall control is not within the scope of this report.

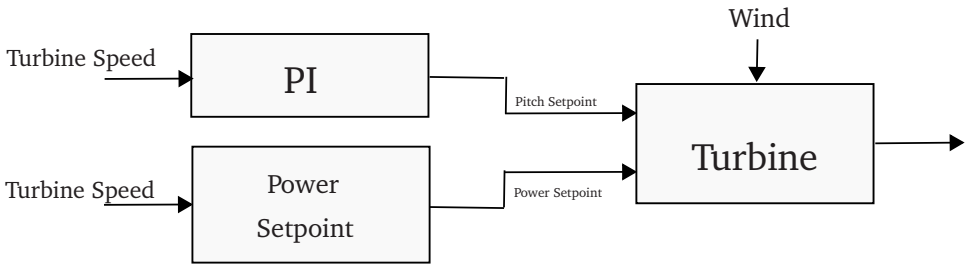

Figure 2.3: A block diagram of a typical wind turbine control system

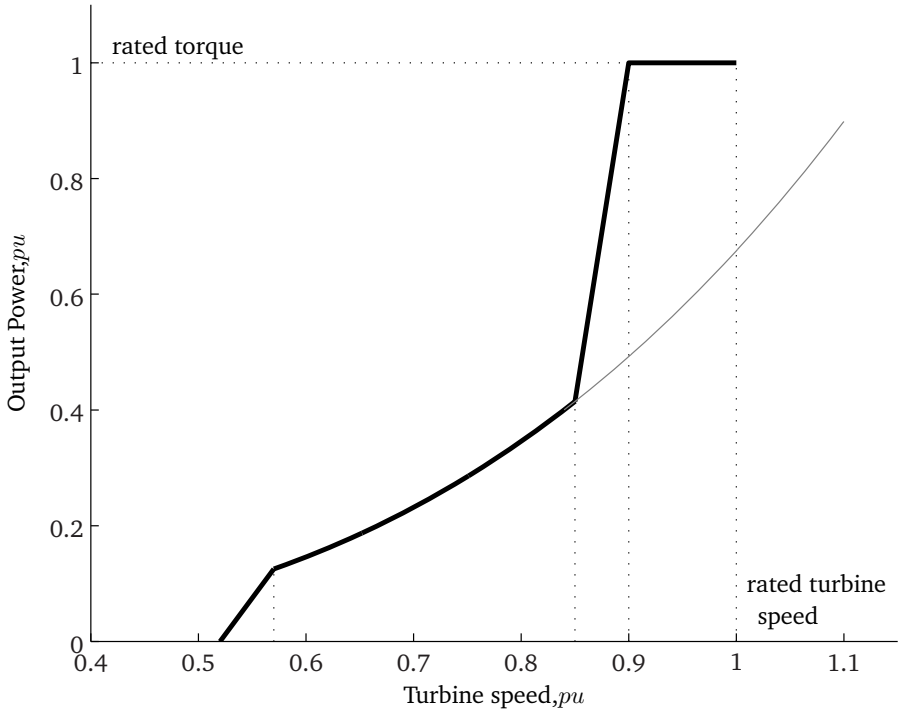

Figure 2.4: Relation between turbine speed and output power in variable speed operation. The breakpoints in the figure can vary for different implementations

2.3 Wind Field Effects

Wind speeds vary over the rotor area. This leads to some effects that are important to be aware of. Because winds are generally stronger at higher altitudes the torque applied on the wind turbine is higher when two blades point upwards (Y-shape) and correspondingly lower when two blades point downwards. This is known as the *wind shear* effect. Wind shear leads to an oscillation with frequency three times the turbine frequency. The fact that the air has to move around the tower leads to a drop in the wind speed in front of the tower. This is called the *tower shadow*.

The large wind turbine area leads to that the total delivered torque is a low-pass-filtered version of the point wind speeds in the swept area. The effect of a wind gust for example will be *damped out* because the gust does not come simultaneously over the hole area.

Wind modeling is the topic of Section 3.2.6.

Chapter 3

Modeling

3.1 Overview

The structure that will be modeled in this thesis is based on a standard 5 MW wind turbine, mounted on top of a floating base. The wind turbine is the 5 MW reference wind turbine for offshore system development defined by the NREL in Jonkman et al. (2009). They introduced this turbine so that results from various research projects on offshore wind energy should be easier to compare. Some basic data on the turbine is given in table 3.1.

Rating	5 MW
Rotor, Hub Diameter	126 m, 3 m
Hub Height	90 m
Cut-In, Rated, Cut-Out Wind Speed	3 m/s, 11.4 m/s, 25 m/s
Cut-In, Rated Rotor Speed	6.9 rpm, 12.1 rpm
Rated Tip Speed	80 m/s
Rotor Mass	110,000 kg
Nacelle Mass	240,000 kg
Tower Mass	347,460 kg

Table 3.1: Main data of the NREL 5-MW reference wind turbine. Jonkman et al. (2009)

The floater is designed as a cylindrical semi-submersible platform, and the dynamic equations are obtained from simulations in a numerical simulation software, WAMIT.

3.2 Simulation Model

A simulation model is developed and implemented in Simulink in order to simulate the system and evaluate the controllers.

A sketch of the wind turbine is shown in Figure 3.1.

3.2.1 Turbine Aerodynamics

A common, basic way of modeling the power from a wind turbine is (see e.g. Manwell et al. (2002))

$$P_w = \frac{1}{2} A \, \rho \, Cp(\lambda, \beta) \, v_r^3 \tag{3.1}$$

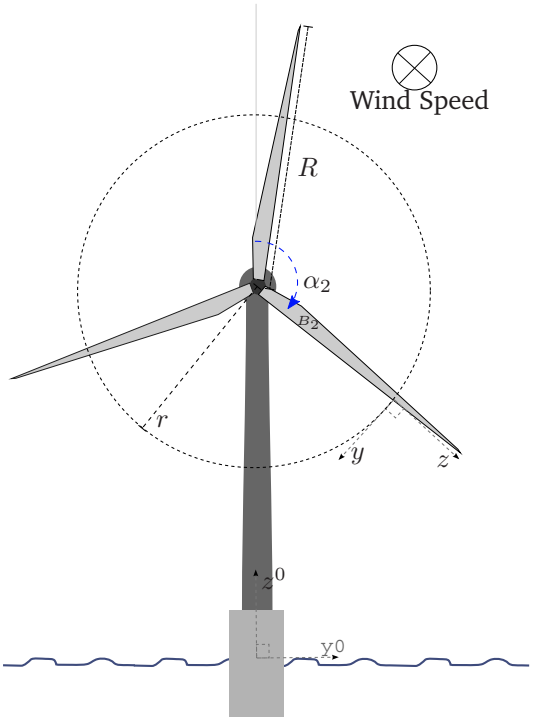

Figure 3.1: Drawing of the wind turbine, seen in the wind direction

where A is the total swept area of the turbine and ρ is the density of air. Cp is the efficiency factor that is dependent on the tip speed ratio, $\lambda = \omega_t \cdot R/v$ and the pitch angle β. v_r is the resulting wind speed for the whole area and ω_t is the turbine rotation speed.

A more advanced modeling approach for wind turbine aerodynamics is to use the blade element method(BEM). That entails dividing the blades into many small segments, assume constant conditions for each segment, and calculate the lift, drag etc. for each segment. This method gives the most accurate simulations, but is also a more complex strategy.

This report does not aim to design a state-of-the-art simulator, but the modeling will compromise between the two modeling approaches mentioned above. The simulator will have independent blades, and will include blade flapping in two degrees of freedom. Wind phenomena such as wind shear and tower shadow will also be taken into account. BEM will not be used.

The torque applied on each blade will be calculated like in (3.1), but with independent pitch angle, and effective wind speed. The aerodynamics of each blade is computed at one point, p_r, on each blade situated such that in steady wind conditions the same amount of torque is applied to the blade inside and outside of this point(see Fig. 3.1). By inserting in (3.1) we get

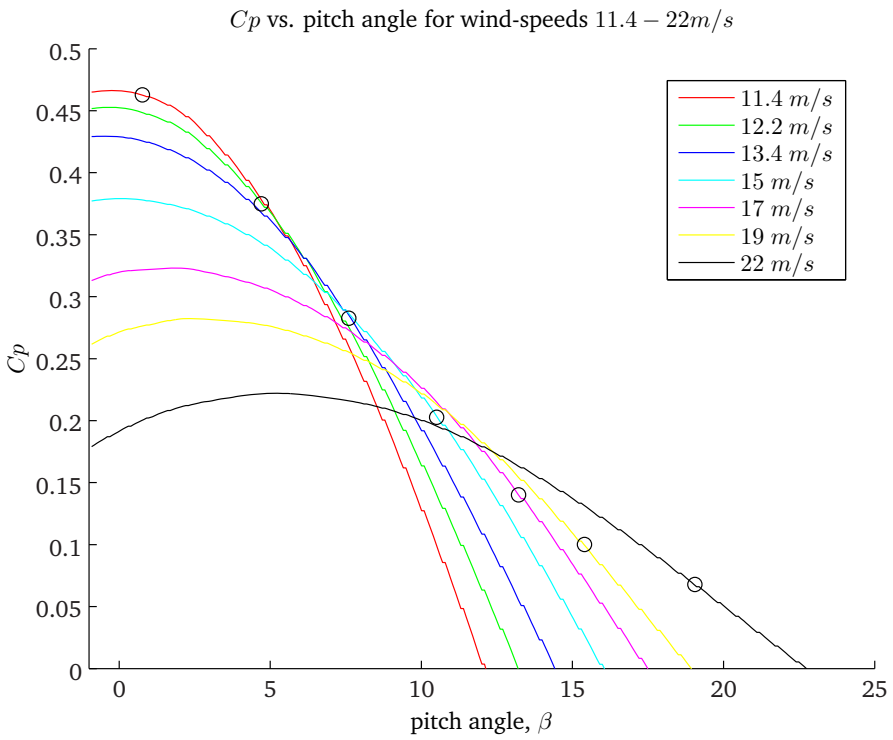

Figure 3.2: Torsional efficiency factor as a function of pitch angle for different wind speeds. 'o' indicates the pitch angle that gives rated output power for different operating points

$$P_w(r) = \frac{1}{2} P_w(R) \tag{3.2}$$

$$\frac{1}{2}\,\pi\, r^2\,\rho\, Cp(\lambda,\beta)\, v^3 = \frac{1}{2}\left(\frac{1}{2}\,\pi\, R^2\,\rho\, Cp(\lambda,\beta)\, v^3\right) \tag{3.3}$$

$$r^2 = \frac{1}{2} R^2 \tag{3.4}$$

$$r = \frac{R}{\sqrt{2}} \tag{3.5}$$

By using an approach to modeling like in (3.1) all details about the aerodynamics are hidden in the factor $Cp(\lambda,\beta)$. Cp, the torsional efficiency factor, is a nonlinear map from the tip speed ratio, λ, and blade pitch angle, β. The Cp-value for different tip speeds, varying with pitch angle can be seen in Figure 3.2 [1] . By calculating this for each of the blades at the point r the simple aerodynamic model is extended to include independent blades.

The torque delivered from the i-th blade is

$$T_{b_i} = \frac{1}{3}\left(\frac{1}{2} A\rho\, Cp(\lambda_{ri},\beta_i)\, v_{ri}^3\right) \tag{3.6}$$

where λ_{r_i} is the lambda value calculated at the distance r from the hub for the i-th blade, and v_{ri} is the effective wind speed at the same point. β_i is the individual pitch angle for the i-th blade.

[1] Values for Cp is courtesy of Sintef Energy Systems for a standard wind turbine blade.

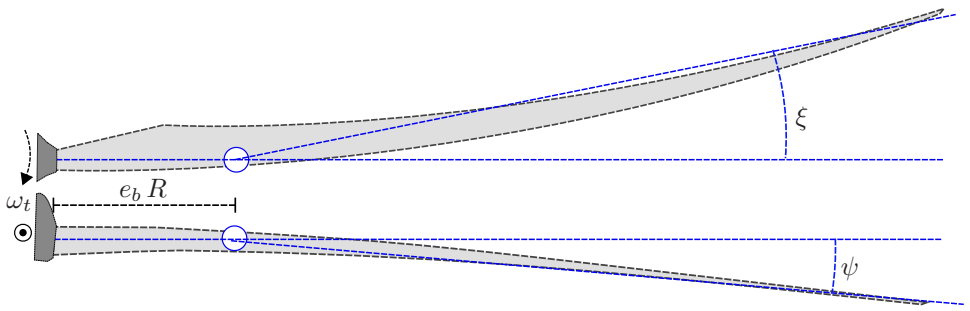

Figure 3.3: Illustration of the bending blade and the equivalent hinge (blue)

3.2.2 Blade Motion

The blades will be modeled with two degrees of freedom. They bend in-plane, or edgewise, and out-of-plane or flap-wise. The blade can according to Eggleston & Stoddard (1987) be modeled as a hinged beam as shown in Figure 3.3. The hinge is placed a distance $e_b \cdot R$ out from the hub, and the two blade sections are considered stiff. It is assumed that there are no torsional vibrations in the blade, and that the two degrees of freedom are strictly in-plane and out-of-plane regardless of the pitch angle. e_b is decided from the vibration frequencies of the blade and these are given in the NREL reference turbine definition.

According to Eggleston & Stoddard (1987) can the blade movement be described by the following dynamic equations.

Flap-wise (out-of-plane):

$$\ddot{\psi} = -\left(\omega_t^2(1+\epsilon) + G\cos\alpha + \frac{K_\psi}{I_b}\right)\psi + \frac{M_\psi}{I_b} \tag{3.7}$$

where ψ is the flapping angle at the hinge, ω_t is the turbine speed and $\epsilon = 3e_b/2(1-e_b)$ is a hinge factor. $G\cos\alpha$ is the moment from gravity, I_b is the blade second mass moment of inertia about the root and K_ψ is the hinge spring constant. M_ψ is the moment from the wind forces given by

$$M_\psi = F_d r \tag{3.8}$$

Where F_d is the drag force on each blade given by Manwell et al. (2002) as

$$F_{d_i} = \frac{1}{3}\left(\frac{1}{2}A\;\rho\;Ct(\lambda,\beta)\;v_{r_i}^2\right) \tag{3.9}$$

Ct is a drag coefficient depending on the tip-speed-ratio, λ, and the pitch angle, β. In the simulations the drag is calculated in a similar fashion as the torque. The Ct-values for different tip-speed-ratios, varying with pitch angle can be seen in Figure 3.4.

Also *in-plane*, *edgewise*, or *lead/lag* vibrations are modeled. Edgewise vibrations can lead to torque fluctuations and oscillations in the drive-train, and could be controllable by adjusting the generator torque and/or the blade pitch angle. The edgewise vibrations can according to Eggleston & Stoddard (1987) be modeled similarly as

$$\ddot{\xi} = -\left(\omega_t^2\epsilon + \frac{K_\xi}{I_b} + G\cos\alpha\right)\xi + 2\,\omega_t\,\psi\,\dot{\psi} - G\sin\alpha + \frac{M_\xi}{I_b} \tag{3.10}$$

ξ is the lead/lag angle at the hinge, K_ξ is the blade spring constant and M_ξ is the moment from the wind forces given by:

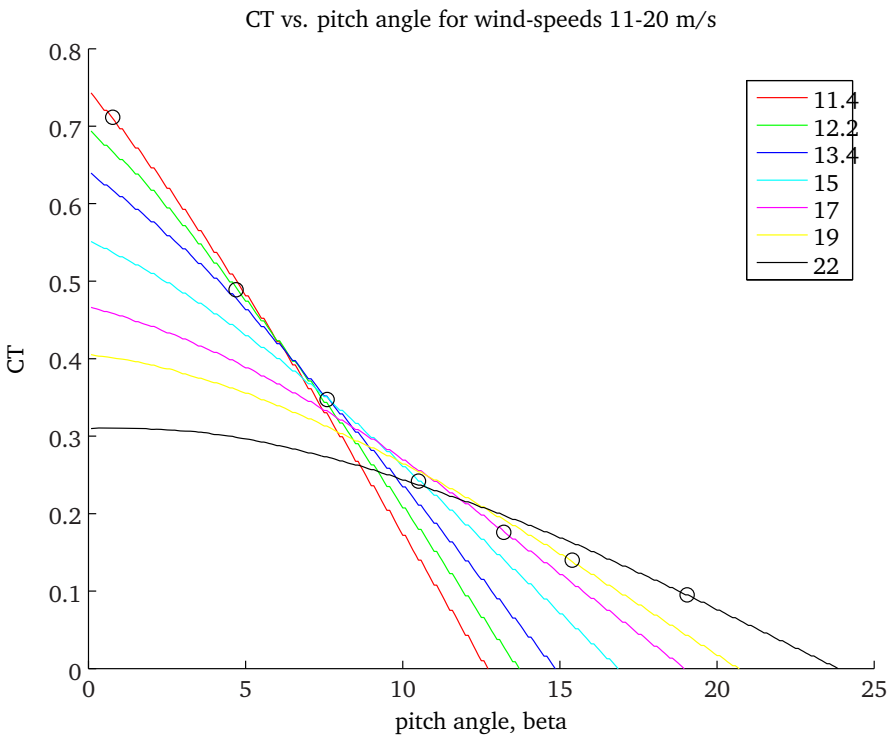

Figure 3.4: Drag force efficiency factor as a function of blade pitch angle for different wind speeds. 'o' indicates the pitch angle that gives rated output power for different operating points

$$M_\xi = T_b(1 - \sqrt{2}\, e_b) \tag{3.11}$$

Where T_b is the torque applied on the blade from the wind given by equation 3.6.

3.2.3 Transmission Modeling

The torque from the wind is applied to the flexible blades, and transmitted to the hub. From the hub, the moment is transmitted through a flexible shaft to the generator. A common way of modeling the transmission in a wind turbine is to see it as a two-mass model Munteanu et al. (2008). A generator mass and a turbine mass is connected by a mass-less spring and damper. In order to incorporate blade motion this model is augmented with one mass for each blade. This leads to the following dynamic system:

Diameter	$5m$
Height	$100m$
Volume	$7853m^2$
Weight	$7200t$
Center of Gravity (incl. turbine)	$-80m$
Eigenfrequency in pitch	$41.3s$

Table 3.2: Main data of the modeled floater

$$\dot{\omega}_s = \frac{1}{2\,H_e}\left(K_s\theta + D_s(\omega_t - \omega_e) - \frac{P_{set}}{\omega_e}\right) \tag{3.12}$$

$$\dot{\theta} = \omega_t - \omega_e \tag{3.13}$$

$$\dot{\omega}_t = \frac{1}{2\,H_t}\left(-K_s\theta - D_s(\omega_t - \omega_e) + \frac{1}{P_n}\frac{K_\xi^*}{1-\sqrt{2}e_{blade}}(\xi_1+\xi_2+\xi_3)\right) \tag{3.14}$$

$$\dot{\xi}_i = \omega_{\xi_i} - \omega_t \tag{3.15}$$

$$\begin{aligned}\dot{\omega}_{\xi_i} = (1-\sqrt{2}\,e_{blade})\frac{1}{I_{blade}}\Big(&- K_\xi^*\xi_i + G\sin\alpha_i \\ &+ \frac{1-\sqrt{2}\,e_b}{6\omega_\xi} A\,\rho\,Cp(\omega_t,\beta_b,\nu,v,\dot{\xi}_i,\dot{\phi})\,v_r^3\Big)\end{aligned} \tag{3.16}$$

where ω_{b_i} is the rotational speed around the hub of blade i, and α_i is the angle of the blade relative to the vertical. According to (3.10) K_ξ^* is given by:

$$K_\xi^* = \left(\omega_t^2\epsilon_2 + \frac{K_\xi}{I_b} + G\cos\alpha\right) \tag{3.17}$$

This approach couples the edge-wise bending of the blades with the rotation of the drive train in a good manner, and is should be a suiting formulation especcially for control purposes.

A schematic drawing of the system is shown in Figure 3.5.

3.2.4 Platform modeling

The wind turbine is mounted on a long slender, cylindrical floater. The floater is very massive, and has a low center of gravity in order to make the entire structure, including the turbine, stable. The cylinder that is used here is designed to resemble the systems proposed by the industry, such as the Hywind project (StatoilHydro (2009)). The basic data for the floater can be found in Table 3.2. Figure 3.6 shows a sketch of the floater.

In order to obtain a six degrees-of-freedom(DOF) model the platform is modeled in WAMIT. WAMIT is a high end numerical potential theory program that can produce the vessel's dynamic equations and the wave response of the vessel. The input to WAMIT is the size, shape and weight of the structure, and it produces a frequency independent dynamic model of the vessel and the interaction with waves and currents.

With the output from Wamit a model can be obtained on the form

$$M\dot{\nu} + C(\nu)\nu + D(\nu)\nu + g(\eta) + g_0 = \tau_{wind} + \tau_{waves} \tag{3.18}$$

$$\dot{\eta} = J(\eta)\nu \tag{3.19}$$

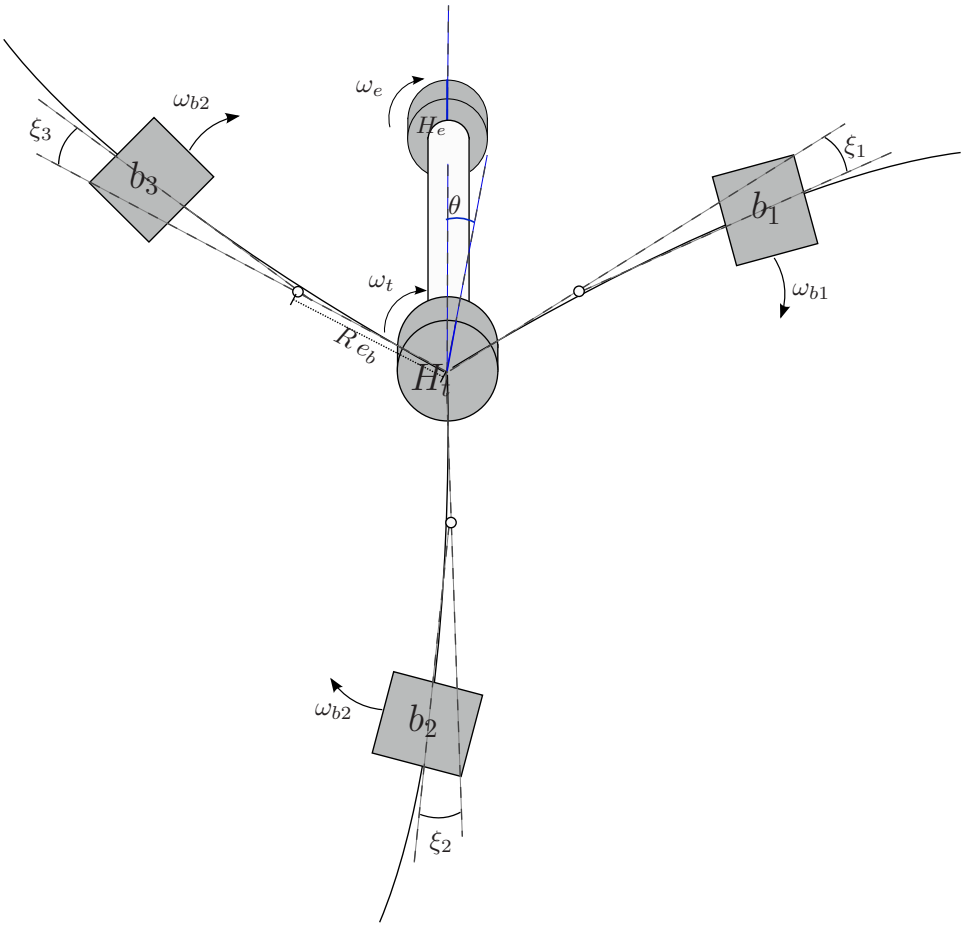

Figure 3.5: Schematic drawing of the five mass model of the wind turbine. H_t, H_e and b_i are the inertias of the hub, the generator and the blades respectively. θ is the shaft lag angle, and ξ_i is the lag angle of the blades. ω_t, ω_e and ω_{b_i} are the rotational speeds of the hub, the generator and each blade respectively.

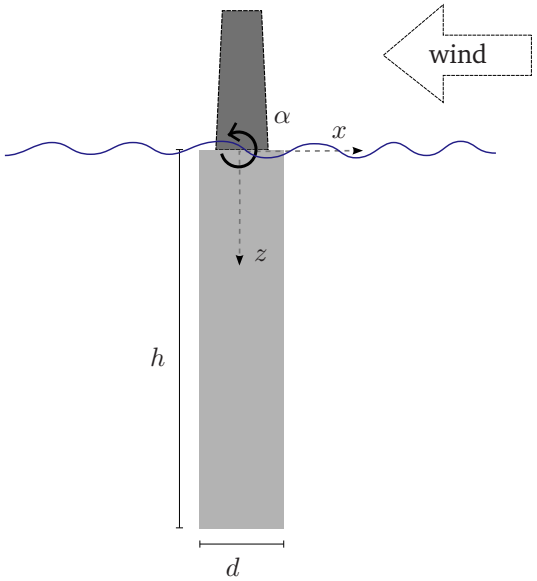

Figure 3.6: Sketch of the floater for the wind turbine

where $\eta = [x\, y\, z\, \Phi\, \Theta\, \Psi]^\top$ is the position in six degrees-of-freedom (DOF) and $\nu = [u\, v\, w\, p\, q\, r]^\top$ [2] is the linear and angular velocities. τ_{wind} is the drag forces from the wind turbine, and they can according to Manwell et al. (2002) be modeled as:

$$F_d = \frac{1}{2} A\, \rho\, Ct(\lambda, \beta)\, v_r^2 \tag{3.20}$$

This gives the drag force from the i-th blade. This is the same equation as (3.9).

$$F_{di} = \frac{1}{3}\Big(\frac{1}{2} A\, \rho\, Ct(\lambda_i, \beta_i)\, v_{ri}^2\Big)$$

g_0 in (3.19) includes linear restoring forces from the anchors of the turbine.

Note: The platform model and the wave influences are modeled in all 6 DOFs. This is not the case for the turbine, which is assumed to be perfectly aligned with the wind direction at all times.

3.2.5 Induced Motions by Blade and Tower Movement

The tower motion and the blade motion induces movement at the blades that leads to a change in the experienced wind speed. The experienced vind speed will then be given by

$$v_r = v + v_{ind} \tag{3.21}$$

Tower motion The tower motion is described by ν and η. They are, according to the SNAME notation (Fossen (2009)), defined with a negative z-axis

The location of the point p_r on each blade (3.5) is defined by the tower position, η, and the rotational angle of the blade, α. The position of p_r relative to the platform is

$$p_r^p = R_p^b(\alpha)\, p_r^b + p_n^p = \begin{bmatrix} 1 & 0 & 0 \\ 0 & \cos\alpha & -\sin\alpha \\ 0 & \sin\alpha & \cos\alpha \end{bmatrix} \begin{bmatrix} 0 \\ 0 \\ r \end{bmatrix} + \begin{bmatrix} 0 \\ 0 \\ h \end{bmatrix} \tag{3.22}$$

where the subscripts p, n and b denotes the platform, nacelle and blade, respectively.

The position of p_r relative to the inertial system is

$$p_r^0 = R_p^0\, p_r^p(\eta) \tag{3.23}$$

$$= R_p^0(\eta)\, \big(R_p^b(\alpha)\, p_r^b + p_n^p\big) \tag{3.24}$$

According to Spong et al. (2006) the linear velocity of the point p_r is given by

$$\dot{p_r^0} = \dot{R}_p^0\, p_r^p + \dot{o}_p^0 \tag{3.25}$$

$$= S(\nu)\, R_p^0(\eta)\, p_r^p(\alpha) + \dot{o}_p^0(\nu) \tag{3.26}$$

Ultimately, to calculate the aerodynamics, we want to have the velocity relative to the inertial frame in blade coordinates. (x-axis up-wind, z-axis along the blade)

$$\nu_{p_r}^b = R_p^0 R_p^b(\alpha) \dot{p_r^0} \tag{3.27}$$

[2] In the rest of the thesis ν and η will be used, but the other terms are not reserved. In particular r, v and Ψ are used with another meaning

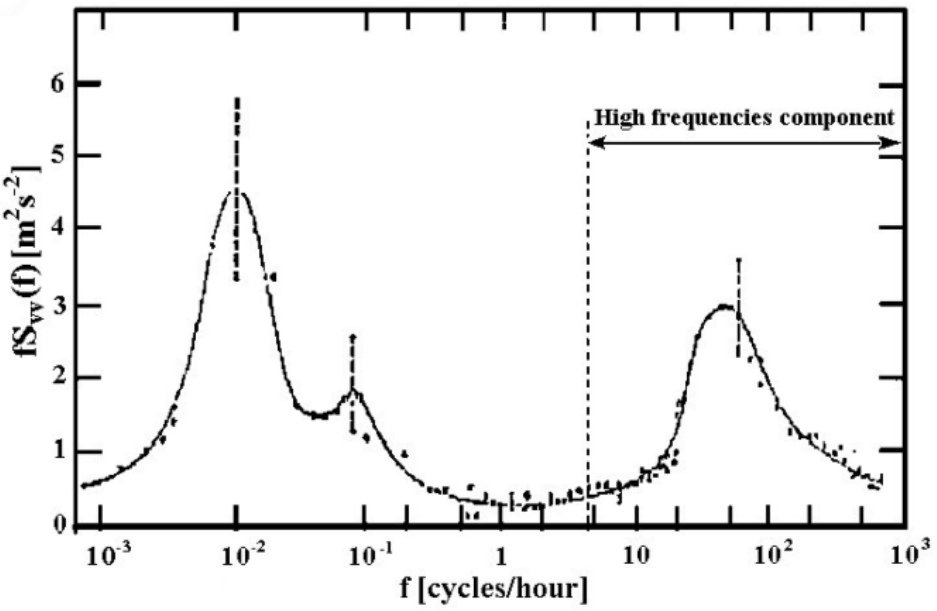

Figure 3.7: The Van Der Hoven wind spectrum. Figure from Nichita et al. (2002)

The x-component of this vector is in the wind direction and a positive speed leads to an increase in the experienced wind speed. The y-component leads to an increase in the experienced turbine speed that is used to calculate the λ-value in equations (3.6) and (3.9). The z-component of the speed-vector can be neglected.

Blade Flapping Flapping of the blades also leads to a change in the experienced wind speed. The dynamics of the blade vibrations are shown in Chapter 3.2.2.

Again, we want to obtain the movement of the point p_r on the blade. We remember that the point r is located a distance $R/\sqrt{2}$ from the hub (3.5), and that the equivalent hinge that the blade vibrates about is located $R\,e_b$ from the hub. The out-of-plane speed of the blade due to flapping is then

$$\dot{p}_{r_x}(\psi) = \dot{\psi}\,(r - R\,e_b) \tag{3.28}$$

where p_r is the calculation point for each blade and $\dot{p}_{r_x}$ denotes the linear velocity of this point in the x-direction.

The movement due to the edgewise flapping is already included in the model, as the λ-values in (3.6) are calculated with ω_ξ.

3.2.6 Wind Modeling

The wind is obviously an important factor when modeling a wind turbine. The wind speed at a given point varies stochastically but with a known frequency spectrum. According to for example the *Van der Hoven spectrum* (Bianchi et al. (2005)) the frequency spectrum of the wind can be separated into a low frequency component and a high frequency component - turbulence. The Van der Hoven spectrum is shown in Figure 3.7. Turbulence is considered frequencies with a shorter period than 10 minutes, and from a control perspective we can therefore model the wind as a sum of a constant wind speed and the turbulence.

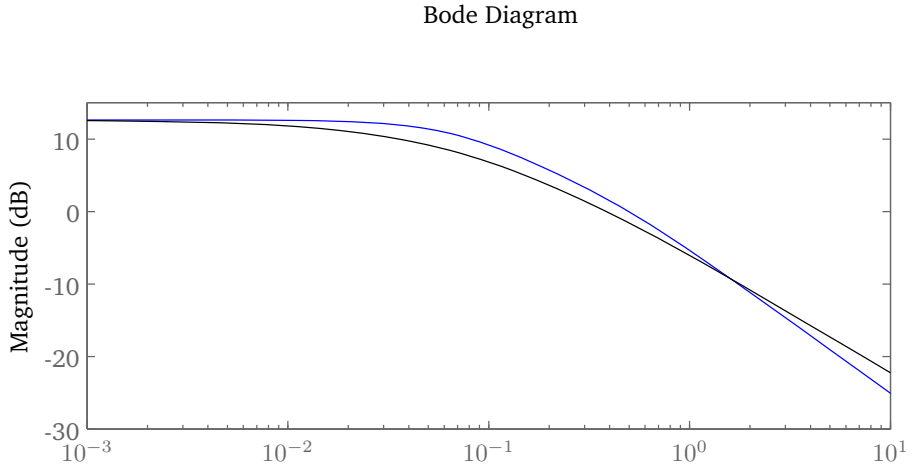

Figure 3.8: Bode plot of the von Karmal filter (3.30),black and the rational approximation (3.32), blue)

$$v = \bar{v} + v_{trb} \tag{3.29}$$

The turbulent wind is not well described by Van der Hoven's model (Munteanu et al. (2008)), because this gives turbulence of the same magnitude regardless of the mean wind speed. A better description is given by the *von Karmal spectrum*. According to Nichita et al. (2002) a wind series, true to the von Karmal model is generated by feeding zero-mean white noise through a shaping filter given by

$$H_v = \frac{K_f}{(1 + s\,Tf)^{5/6}} \tag{3.30}$$

where $T_f = L_{trb}/\bar{v}$ is a time-constant, L_{trb} is a site-specific turbulence length and K_f is given by

$$K_f = \sqrt{\frac{2\pi}{\mathbf{B}(\frac{1}{2}, \frac{1}{3})} \frac{T_F}{T_s}} \tag{3.31}$$

where $\mathbf{B}$ is the beta-function Weisstein (n.d.) and T_s is the sampling time for the wind series.

(3.30) is not a rational transfer function and Nichita et al. (2002) suggests a second order approximation:

$$\hat{H}_v = K_f \frac{m_1 T_f s + 1}{(Tfs + 1)(m_2 T_f s + 1)} \tag{3.32}$$

where m_1 and m_2 are constants given to be 0.4 and 0.25 respectively. Bode plots of the von Karmal filter (3.30) and the rational second-order approximation (3.32) are shown in Figure 3.8.

The turbulence intencity, I_{trb}, describes how strong the variations in the wind speed are, and is defined as

$$I_{trb} = \frac{\sigma}{\bar{v}} \tag{3.33}$$

where σ is the standard deviation of the turbulence component, v_{trb}.

The point wind turbulence is described by the above explanations but the wind speed variations are also spatial. To include these spatial variations four different point wind speeds are generated across the rotor area, and interpolation is used to

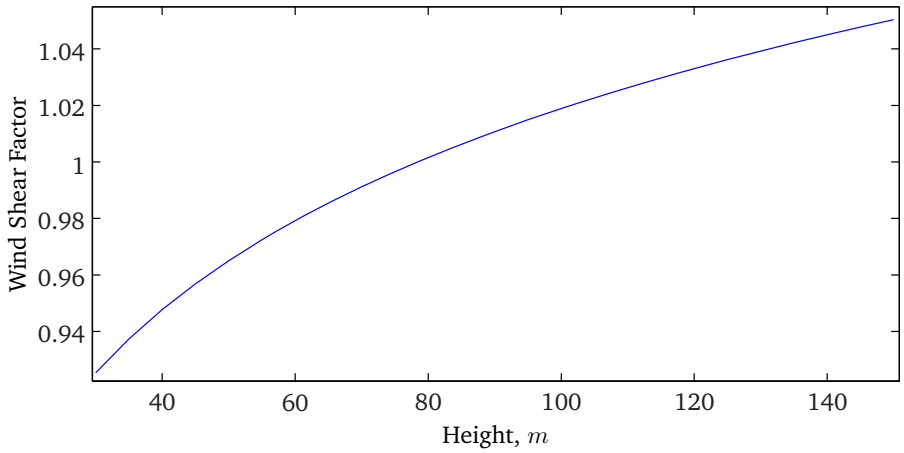

Figure 3.9: Wind Shear Factor. The deterministic wind speed as a factor of the mean wind at nacelle level due to wind shear.

find the wind speed at all points. Each of the four point wind series are generated by adding two wind series - one common for the whole wind area, and one independent wind series. This procedure is designed in discussions with Sintef Energy Research.

In the Matlab simulations two additional effects are modeled; *Wind Shear* and *Tower Shadow*. Wind Shear is the fact that the wind speed is slower closer to the ground due to friction with the ground. According to DWIA (2003) the wind shear effect can be modeled as

$$v(z) = v_0 \frac{ln(\frac{z}{z_0})}{ln(\frac{z_n}{z_0})} \tag{3.34}$$

Where v_0 is the wind speed at some nominal height, z_n (e.g. the hub height), and z_0 is the so-called roughness length for the turbine location. DWIA (2003) gives a value for the roughness length of a water surface to be 0.0002 m. This gives the wind shear factor curve presented in Figure 3.9.

Also, the air is forced to the sides in front of the tower. This leads to a drop in wind torque as the blade passes the tower. This is known as the *tower shadow*. According to Bianchi et al. (2007) the axial wins speed can be modeled as:

$$v_x = \begin{cases} v\left(\frac{R_t^2}{d_{ts}^2}\right)\cos 2\phi & \pi/2 \leq \alpha < -\pi/2 \\ v & -\pi/2 \leq \alpha < \pi/2 \end{cases} \tag{3.35}$$

where R_t is the tower radius, d_{ts} is the distance from the particular point of the blade to the center of the tower and ϕ is the angle between point of the blade and the airflow direction. The effect of the tower shadow is shown in Figure 3.10.

The two deterministic wind speed variations presented above causes a periodic variation in the observed wind speed with a dominating frequency equal to the rotation frequency. The actual frequency response also includes higher harmonics of the rotational frequency, but Munteanu et al. (2008) suggests a filter that approximates the frequency response including the first harmonic of the rotational frequency.

$$H_{v_r}(s) = H_v(s)\, H_{rot}(s) \tag{3.36}$$

$$H_{rot}(s) = \frac{(s + N_b\omega_t + \epsilon)(s + N_b\omega_t - \epsilon)}{(s+\zeta)^2 + (N_b\omega_t)^2} \tag{3.37}$$

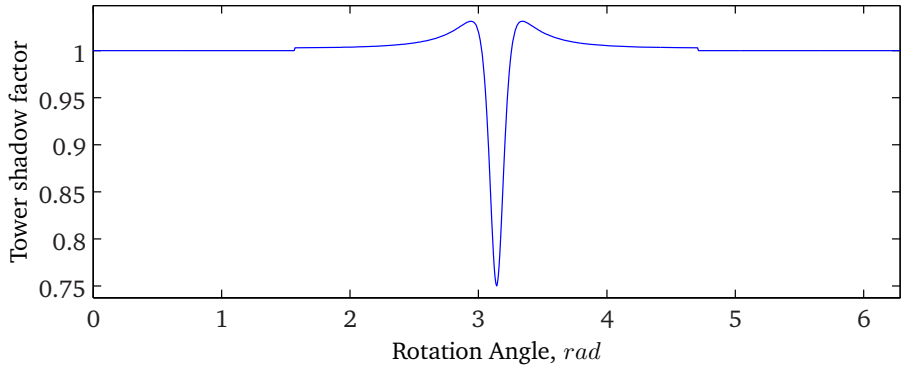

Figure 3.10: Tower Shadow Factor. The deterministic wind speed as a factor of the mean wind at nacelle level due to tower shadow

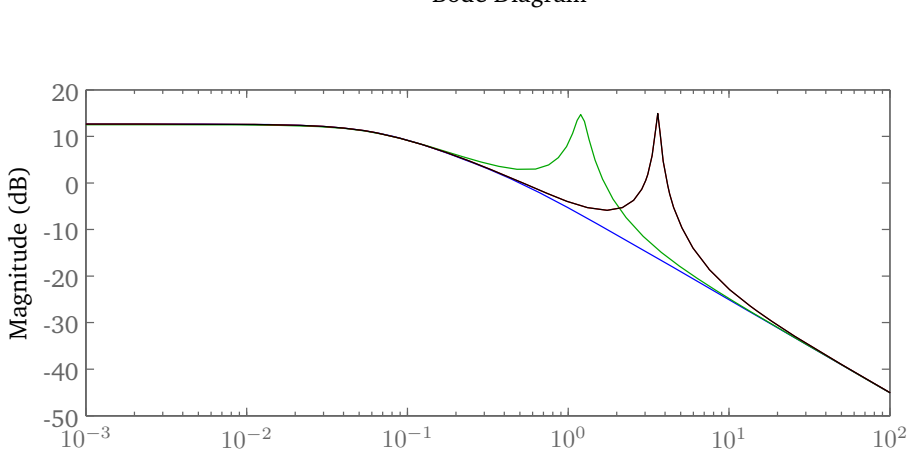

Figure 3.11: Frequency response of the relative wind speed. $H_v(s)$ (blue), $H_{v_r}(s)$ for a single blade (green), for three blades (black).

where $H_v(s)$ is the wind spectrum presented in 3.32, N_b is the number of blades, and ϵ and ζ are design parameters. By choosing N_b as 3 we get the frequency response of the total torque, and $N_b = 1$ gives the frequency response of the wind variations on a single blade. $H_{v_r}(s)$ for one and three blades is shown in Figure 3.11 together with $H_v(s)$.

In this thesis the wind turbine is assumed to be perfectly aligned with the wind direction at all times, and the yaw dynamics of the turbine and effects of side wind or bad allignment is not treated.

3.2.7 Wind Estimation

Obtaining an estimate of the current wind speed can be very useful in the controller design. If linear controllers are used it is necesarry to change the controller parameters according to the operating point, and this operating point can be described by the wind speed. In the following, a simple scheme for estimating the incoming wind power based on other system values is developed.

If tight control of the oscillations in the drive train and blades is implied - $\omega_t = \omega_e = \omega_\xi$ - a simpler one-mass model can be developed. By combining (3.12)-(3.16) we get

$$\dot{\omega} = \frac{1}{H^*}\left(T_w - T_e\right) \tag{3.38}$$

$$H^* = 2H_t + 2H_e + 3\frac{I_{blade}}{(1-\sqrt{2}\,e_{blade})} \tag{3.39}$$

Where T_w and T_e is the torque from the wind and the generator respectively. By rewriting we get

$$T_w = T_e + H^*\,\dot{\omega} \tag{3.40}$$

$$\frac{1}{2}A\rho\,Cp(\lambda,\beta)\,v^3 = P_e + H^*\,\omega\dot{\omega} \tag{3.41}$$

$$v^3 = \frac{P_e + H^*\,\omega\dot{\omega}}{\frac{1}{2}A\,\rho\,Cp(\lambda,\beta)} \tag{3.42}$$

This gives the final expression

$$v = \sqrt[3]{\frac{P_e + H^*\omega\dot{\omega}}{\frac{1}{2}A\rho\,Cp(\lambda,\beta)}} \tag{3.43}$$

It should be noted that calculating this requires good measurements and/or estimates of the states in the system. The differentiation of the measurement of ω is not ideal, but overcoming this should not be a big problem. Similar wind estimates are used in e.g. Skaare (2009) and Nichita et al. (2002).

3.2.8 Wave Modeling

The wave model that is used in the simulator is based on Wave Force Response Amplitude Operators (RAO) as described in Fossen (2009). They are computed with the hydrodynamic program WAMIT together with the floater's dynamic equations (see Sec. 3.2.4). The RAO's can includes both 1st and 2nd order wave induced loads on the vessel, but only 1st order forces are modeled here.¨

The waves follow the Jonswap spectrum, that characterizes the waves in the north sea. The forces on the vessel from the waves can be aproximated by (Fossen (2002)):

$$\tau_{wave} \approx \mathbf{K}_w\,H(s)\,w(s) \tag{3.44}$$

where $\mathbf{K}_w$ is a gain matrix, and $w(s)$ is zero-mean white noise. $H(s)$ is a linear filter that includes the wave spectrum

$$H(s) = \frac{s}{s^2 + 2\lambda\omega_0 s + \omega_0^2} \tag{3.45}$$

$\mathbf{K_w}$ is given by $diag(k_{w1}k_{w2}\ldots k_{w6})$ and

$$k_{wi} = 2\lambda\omega_0\sigma \tag{3.46}$$

σ is a scaling constant.

The gains in the linear model are tuned to fit with simulation results from the RAO-model.

In the simulations the wave height is given from the mean wind speed and the Beaufort scale. The peak frequency, ω_0, is chosen to be $0.8rad/s$ as proposed in Fossen (2009).

It is important to note that the common wave frequencies are higher than the eigenfrequency of the tower.

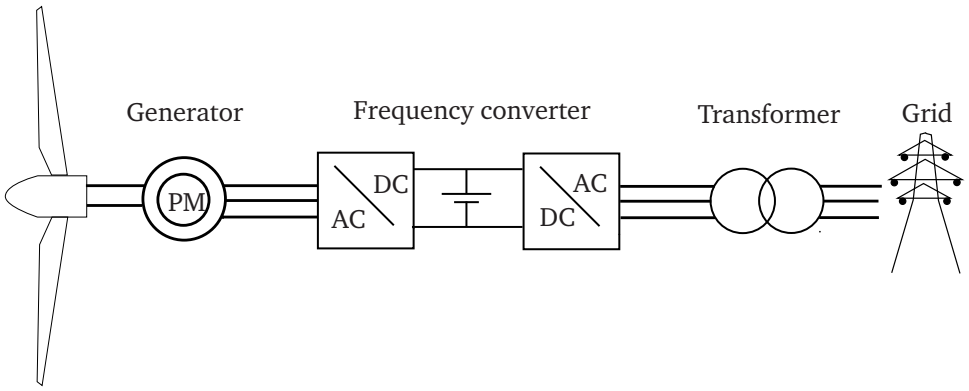

Figure 3.12: Sketch of the PMSG generator and frequency conversion system

3.2.9 Generator Modeling

The generators in the offshore wind turbines discussed here will be Permanent Magnet Synchronous Generator(Hansen & Michalke (2008)). The generator and the frequency converter that controls it are not modeled in this thesis, but a sketch is presented in Figure 3.12. The dynamics of these generators are assumed to be much faster than the drive train dynamics. Chincilla et al. (2006)) indicates that the power control system gives settling times of around $0.01s \rightarrow f \approx 100Hz$. For the slower dynamics of the wind turbine we can therefore assume.

$$P_e = P_{set} \tag{3.47}$$

3.2.10 Pitch Dynamics

The pitch actuator is modeled as a simple, fast first order system.

$$\dot{\beta} = \frac{1}{T_\beta}(\beta_d - \beta) \tag{3.48}$$

where β_d is the pitch angle set point. T_β is chosen as $0.5s$.

3.3 Control Model

For control purposes a linear model is necessary. The nonlinear simulation model developed in the previous section is rather expansive and for the linear model to have a reasonable size, it is necessary to do some simplifications. The control model will be focused on the dynamics that can be affected by control.

The five-mass model described in section 3.2.3 will be linearized and included in the model, while the flapping will be left out of the control model. The reduced model will have four control inputs - One for each blade pitch set point and one for the generator set point. The 6 DOF model of the floater will be reduced to 3 DOFs, namely surge, heave and pitch. The wind speed at each blade is considered a disturbance and so is the wave influence. This will lead to the following state, input and disturbance vectors.

$$x = [\omega_t \ \omega_e \ \theta \ \beta_1 \ \beta_2 \ \beta_3 \ \xi_1 \ \xi_2 \ \xi_3 \ \omega_{xi_1} \ \omega_{xi_2} \ \omega_{xi_3} \ \hat{\eta} \ \hat{\nu}]^\top \tag{3.49}$$

$$u = [\beta_{set_1} \ \beta_{set_2} \ \beta_{set_3} \ P_{set}]^\top \tag{3.50}$$

$$v = [v_1 \ v_2 \ v_3 \ v_{wave}]^\top \tag{3.51}$$

3.3.1 Reduction of Vessel Model

The nonlinear dynamic equation for the floater dynamics is given in equation 3.19. By utilizing the small deflections and velocities of the wind turbine a linear model can be obtained.

Assuming small angles ($\phi, \theta \approx 0$) allows the use of vessel parallel coordinates (Fossen (2009)).

$$\eta_p = P^\top(\psi) \ \eta \tag{3.52}$$

where $P(\psi)$ is given by

$$P(\psi) = \begin{bmatrix} R(\psi) & 0_{3\times3} \\ 0_{3\times3} & I_{3\times3} \end{bmatrix} \tag{3.53}$$

This gives

$$\dot{\eta} = J(\eta)\nu \approx P(\psi)\nu \tag{3.54}$$

By further assuming low speed we can obtain

$$\dot{\eta_p} \approx \nu \tag{3.55}$$

this gives

$$\ddot{\eta_p} \approx \dot{\nu} = M^{-1}\left(-C(\nu)\nu - D(\nu)\nu - g(\eta) - g_0 + \tau + \tau_{wind} + \tau_{waves}\right) \tag{3.56}$$

This equation has two non-linear terms left, $g(\eta)$ and τ. $g(\eta)$ can be linearized using VP coordinates:

$$g(\eta) \overset{\phi=\theta=0}{\approx} P^\top(\psi)G\eta = \underbrace{P^\top(\psi)GP(\psi)}_{G}\eta_p = G\eta_p \tag{3.57}$$

This gives us the following equation.

$$\ddot{\eta_p} \approx \dot{\nu} = M^{-1} - C(\nu)\nu - D(\nu)\nu - G\eta_p - g_0 + \tau \tag{3.58}$$

where τ is the drag forces from the wind and the waves. The drag from wind is included in the model, while the wave forces are treated as a disturbance.

The model is then reduced to 3 DOFs by assuming that the other states are zero ($y = \phi = \psi = 0$).

This gives:

$$\dot{\hat{\eta}}_p = \begin{bmatrix} \dot{x} \\ \dot{z} \\ \dot{\Theta} \end{bmatrix} = \hat{\nu} \tag{3.59}$$

$$\dot{\hat{\nu}} = \begin{bmatrix} \ddot{x} \\ \ddot{z} \\ \ddot{\Theta} \end{bmatrix} = \hat{M}^{-1}\left(-\hat{D}\nu - G\hat{\eta}_p + \tau_{wind} + \tau_{wave}\right) \tag{3.60}$$

τ_{wind} is a result of the forces from wind given by equation 3.20 and is

$$\tau_{wind} = \begin{bmatrix} F_{d1} + F_{d2} + F_{d3} \\ 0 \\ h(F_{d1} + F_{d2} + F_{d3}) \end{bmatrix} \tag{3.61}$$

The induced wind speed due to the rotational motion of the nacelle is not included in the linear model, because the blade rotation angle, α, is not. Only the induced movement at the hub is calculated. Small angles are assumed, and the expression for the resulting wind due to tower movement is:

$$v_r = v - h\,\dot{\Theta} + \dot{x} \tag{3.62}$$

3.3.2 Reduction of the Blade Model

As mentioned the blade flapping is not included in the linear model, and thus the coupling terms between the two flapping modes are not included.

The edgewise movement is included as described in (3.12)-(3.16). However, the blade rotation angle, α is not included, and therefore the gravity term has to be left out. The gravitational forces on the blades are large and leads to a dominant movement of the blades with frequency equal to the rotational frequency. It is clearly not desirable (nor possible) to damp out these fluctuations. This frequency should be filtered out from the measurements when designing the controller. This can be done with a band-stop filter filtering out the rotational frequency, or with a feed forward connection from the blade angle

3.3.3 Resulting Linear Model

The remaining linearization is done by partially differentiating the total set of equations. The complete set of equations is

$$\dot{\mathbf{x}} = f(\mathbf{x}, \mathbf{u}, \mathbf{w}) \tag{3.63}$$

where $\mathbf{x} = [\omega_e\ \theta\ \omega_t\ \xi_1\ \xi_2\ \xi_3\ \omega_{xi_1}\ \omega_{xi_2}\ \omega_{xi_3}\ \beta_1\ \beta_2\ \beta_3\ \hat{\eta}\ \hat{\nu}]^\top$, $\mathbf{u} = [\beta_{ref1}\ \beta_{ref1}\ \beta_{ref1}\ P_{set}]$ and $\mathbf{w} = [v_{b1}\ v_{b2}\ v_{b3}]$.

$$f(\mathbf{x}, \mathbf{u}, \mathbf{w}) = \begin{bmatrix} \frac{1}{2\,H_e}\left(K_s\theta + D_s(\omega_t - \omega_e) - \frac{P_{set}}{\omega_e}\right) \\ \omega_t - \omega_e \\ \frac{1}{2\,H_t}\left(-K_s\theta - D_s(\omega_t - \omega_e) + \frac{1}{\omega_t P_n}\frac{K_\xi^*}{1-\sqrt{2}e_{blade}}(\xi_1 + \xi_2 + \xi_3)\right) \\ \omega_{\xi_1} - \omega_t \\ \omega_{\xi_2} - \omega_t \\ \omega_{\xi_3} - \omega_t \\ (1-\sqrt{2}\,e_b)\frac{1}{I_b}\left(-K_\xi^*\xi_1 + \frac{1-\sqrt{2}\,e_b}{6}A\,\rho\,Cp(\omega_{\xi_1}, \beta_1, \nu, v)\,v_{r_1}^3\right) \\ (1-\sqrt{2}\,e_b)\frac{1}{I_b}\left(-K_\xi^*\xi_2 + \frac{1-\sqrt{2}\,e_b}{6}A\,\rho\,Cp(\omega_{\xi_2}, \beta_2, \nu, v)\,v_{r_2}^3\right) \\ (1-\sqrt{2}\,e_b)\frac{1}{I_b}\left(-K_\xi^*\xi_3 + \frac{1-\sqrt{2}\,e_b}{6}A\,\rho\,Cp(\omega_{\xi_3}, \beta_3, \nu, v)\,v_{r_3}^3\right) \\ \dot{\beta}_1 = \frac{1}{T_\beta}(\beta_{1ref} - \beta_1) \\ \dot{\beta}_2 = \frac{1}{T_\beta}(\beta_{2ref} - \beta_2) \\ \dot{\beta}_3 = \frac{1}{T_\beta}(\beta_{3ref} - \beta_3) \\ \hat{\nu} \\ \hat{M}^{-1}\left(-\hat{D}\nu - G\hat{\eta}_p + \tau_{wind} + \tau_{wave}\right) \end{bmatrix} \tag{3.64}$$

where τ_{wind} is

$$\tau_{wind} = \begin{bmatrix} \sum_{i=1}^{3} \frac{1}{3}\Big(\frac{1}{2}A\ \rho\ Ct(\omega_{\xi_i}, \beta_i, \nu, v_{ri})\ v_{ri}^2 \\ 0 \\ h\sum_{i=1}^{3} \frac{1}{3}\Big(\frac{1}{2}A\ \rho\ Ct(\omega_{\xi_i}, \beta_i, \nu, v_{ri})\ v_{ri}^2 \end{bmatrix} \tag{3.65}$$

the system is the linearized around an operating point $(\mathbf{x}_0, \mathbf{u}_0)$ to achieve

$$\Delta\dot{\mathbf{x}} = \frac{\delta f(\mathbf{x}, \mathbf{u})}{\delta \mathbf{x}}\bigg|_{\mathbf{x}_0, \mathbf{u}_0} \Delta\mathbf{x} + \frac{\delta f(\mathbf{x}, \mathbf{u})}{\delta \mathbf{u}}\bigg|_{\mathbf{x}_0, \mathbf{u}_0} \Delta\mathbf{u} \tag{3.66}$$

Details on the linearization can be found in Appendix A
This results in the linear system

$$\Delta\dot{\mathbf{x}} = A(t)\Delta\mathbf{x} + B(t)\Delta\mathbf{u} + G(t)\Delta v \tag{3.67}$$

where $\Delta\mathbf{x}$ and $\Delta\mathbf{u}$ relates to the full states as

$$\mathbf{x} = \mathbf{x}_0 + \Delta\mathbf{x} \tag{3.68}$$

$$\mathbf{u} = \mathbf{u}_0 + \Delta\mathbf{u} \tag{3.69}$$

3.4 Comments and Challenges With the Model

3.4.1 Linear Analysis

Analysis of the linear system can give insight of the system. First we look at the poles and zeros of the system that are shown Figure 3.13. This shows poles and zeros for the open-loop system linearized around different operating points. From the right figure in Fig. 3.13 it can be seen that the system has an open-loop unstable mode with complex poles in the right half plane, for the two highest wind speeds. This instability is related to torsional oscillations in the drive train, and tells us that the controller should include some damping of the drive train.

By development of the controllability matrix

$$\mathcal{C} = [B\ AB\ A^2B\ \cdots\ A^6B] \tag{3.70}$$

in the operating points and finding that it has full rank indicates that the system is controllable. This is done numerically in Matlab.

3.4.2 Measurements and Estimation

In this thesis it is assumed that all states can be measured. This is not neccesarily true, but the measurement and estimation problem is left for other researchers.

To assess how appropriate this assumption is it could be useful to look at what could actually measured. The Turbine speed, ω_t, and generator speed, ω_e, is measured, and from this the shaft angle, θ, can easily be deduced. Measurements of the pitch angles are also available, and the same should be true for the state of the vessel orientation and movement. To assume perfect measurements of the blade bending is a somewhat more bold claim. However, the blade structures are so large that it should be possible to get a decent measurement of it. From this it should be possible to obtain a fair estimate also of the constructed blade rotatinal speeds, ω_{ξ_i}. The reliability and quality of these estimates will not be concidered here.

The linear system is with the assumption that the full state can be measured of course observable.

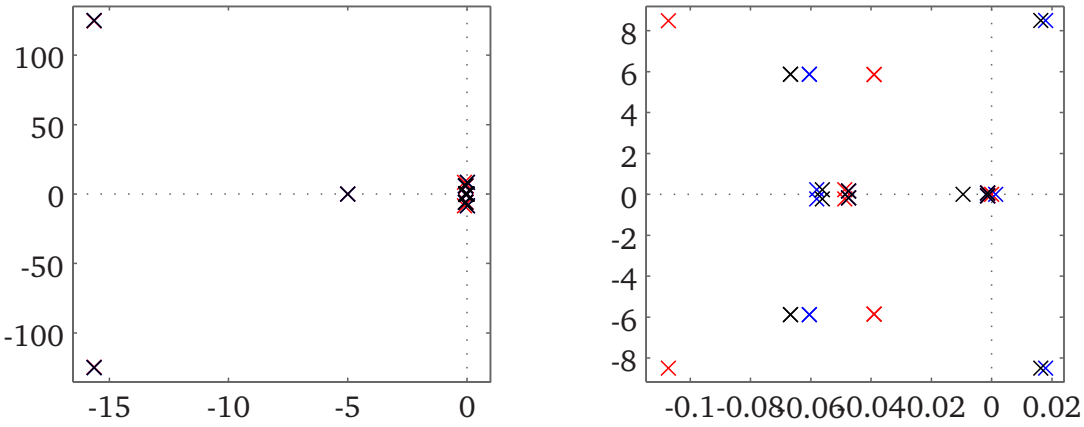

Figure 3.13: Plots of the poles and zeros of the open-loop system linearized around different operating points. Low wind speeds(red), rated wind speed(blue), and high wind speed(black). Poles are marked with 'x', zeros with 'o'. Right plot shows a zoom of the values close to the origin.

3.4.3 Control of Blade Vibrations

A goal in this project was to look into if and how edge-wise blade vibrations could be damped out by control. An initial idea was to reduce the vibrations by means of the generator torque. However it will be pointed out that controlling the blade vibrations is not possible by means of the generator torque alone.

The three blade masses in the 5-mass model (3.12)-(3.16) can be seen as a rotating analogue to an triple inverted pendulum. The *double* inverted pendulum is a classic problem in introductory control theory and one important aspect with this is that it is only controllable if the two pendulums have different masses. In our case the three blades are clearly identical and we cannot control their movement by turning the drive shaft alone.

This can also be shown by finding the controllability matrix of the reduced system and see that it is not full rank. This indicates that individual pitch control is necesarry to reduce blade vibrations.

3.4.4 Positive Feedback of Tower Movement

At high wind speeds the wind turbine enters a power limitation regime to prevent overload in the generator. This power limitation is effectuated by pitch control - increasing the pitch angle to alter the aerodynamics of the blades to reduce the torque applied on the turbine. See (3.1) and Figure 3.2.

This control action also alters the surge force on the tower structure and in the power limitation mode this could lead to negative damping of the tower movement. When the tower oscillates the resulting wind speed (3.21) will vary accordingly. Figure 3.14 shows the surge force on the tower with power limitation as a function of the resulting wind speed. Note the very different behavior below and above rated wind speed.

When the tower moves into the wind, the resulting wind speed increases. Power limitation control leads to increased pitch, that (ref Fig. 3.14) leads to *decreased* force on the tower which again leads to increasing speed. Accordingly, when the tower sway out of the wind the resulting wind speed decreases and this leads to

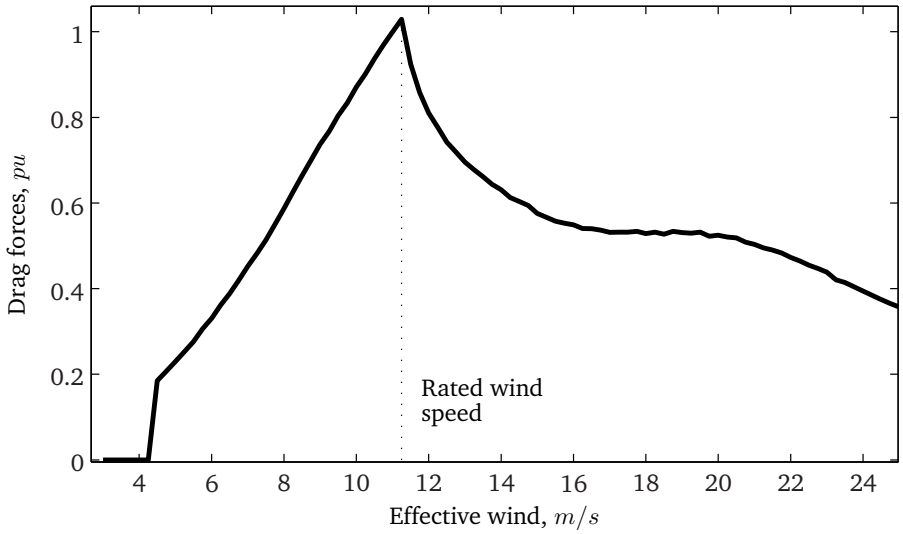

Figure 3.14: Drag force as a function of effective wind speed

increased surge force and increasing speed of the tower. This clearly has to be taken care of with control, and is the main challenge when transforming an on-shore controller to an off-shore application. Solutions to this challenge are treated in Chapter 4.

Chapter 4

Controls

This chapter will go through the development of the control structure of the implemented controllers with focus on a solution using Model Predictive Control. An alternative basic formulation based on a patent by Sintef will be implemented for comparison, an yet another concept based on a different patent will be described but not implemented.

4.1 Control Objectives

There are several control objectives for the wind turbine. In short the goal is to maximize total power output, limit the turbine speed and instantaneous power output to their maximum values, and at the same time reducing all vibrations to increase the fatigue life of the components.

This can be detailed:

- *Limit output power to the rated value.*
  In strong winds the potential power from the wind exceeds the generator power rating. This should be avoided and the output power should, when the wind is strong enough, be equal to the generator power rating - 5MW for the modeled NREL reference turbine.

- *Maintain optimal tip speed ratio*
  The turbine blades are shaped to be most effective at a certain tip speed ratio, and by controlling the turbine speed this optimal tip speed ratio can be maintained for a range of wind speeds - below rated wind power. (See Sec. 2.2.2)

- *Damp out tower oscillations*
  Pitch control above rated wind speed could possibly excite the eigenfrequency of the tower. This should be avoided, and the tower tilt motion should be damped out. (See Sec. 3.4.4)

- *Damp out oscillations in the flexible shaft in the drive train*
  The dynamics of the drive train are soft, and this might lead to instabilities. Oscillations caused by this should be avoided by control.

- *Reduce blade flapping*
  For large wind turbines blade flapping can be a problem, and could reduce the fatigue life of the turbines. It could possibly be reduced by control.

4.2 Model Predictive Control

Model Predictive Control (MPC) is an advanced control method that uses an explicit model of the system to calculate the best control effort. MPC predicts the future behaviour of the system online and chooses the optimal control input from that. MPC can handle constraints on both states and control inputs.

MPC was first developed for use in the chemical industry in the 1980s(Maciejowski (2002)). It was applied to very slow processes and enabled the controllers to use their detailed plant knowledge to decide the control action. Including knowledge about input constraints and measurement noise made it possible to operate closer to the safety constraints, and this could make the operation more profitable.

Because MPC includes online optimization it requires a lot of computational power. This has previously limited the use of MPC to systems with slow dynamics, but this limitation is no longer as applicable. The continuing improvements of the power of computers makes MPC and other controllers involving online optimization an alternative also for faster systems.

An MPC controller's main advantage is the capability to directly handle system constraints on both input parameters and system states, and to include noise models as well as system model.

The Model Predictive Toolbox in MatLab is used to implement the MPC controller for the wind turbine.

4.2.1 MPC Theory

This section will give a short introduction to the concept of linear MPC. The solution described here is the same as used in the *Model Predictive Control Toolbox* in Matlab. MPC is calculated in discrete time, on a discretized version of the model developed in Chapter 3.3.

In this section a discrete system on the common state-space form is assumed

$$x_{k+1} = Ax_k + Bu_k \tag{4.1}$$
$$y_{k+1} = Cx_k + Du_k \tag{4.2}$$

The basic idea is to, at every time step, predict the future system behaviour given the current system state for some future sequence of control inputs. By the use of an optimization technique the control action that minimize some cost function is found. This cost function typically includes state errors and control effort. The control input for the first time step is applied to the function, and the procedure is repeated before the next time step.

Figure 4.1 illustrates the operation of the MPC controller at a time, k. The top plot shows the state, x. The blue line on the left of time k represents the measurements, and the predicted optimal output sequence on the right of time k. The black line represents the actual system state *if the given trajectory is applied*. The reference trajectory is shown in the lower plot. Note that only the first control action, marked with a heavy black line, is actually applied to the system, because the complete procedure is performed again at time $k + 1$. H_c and H_p denotes the control and prediction horizon recpectivly. The control horizon is how many time steps the control action is allowed to vary in the prediction, and the prediction horizon is the number of time steps in the total simulation. Typically $H_p >> H_c$.

A typical cost function is commonly a quadratic one like (van den Boom & Backx (2007))

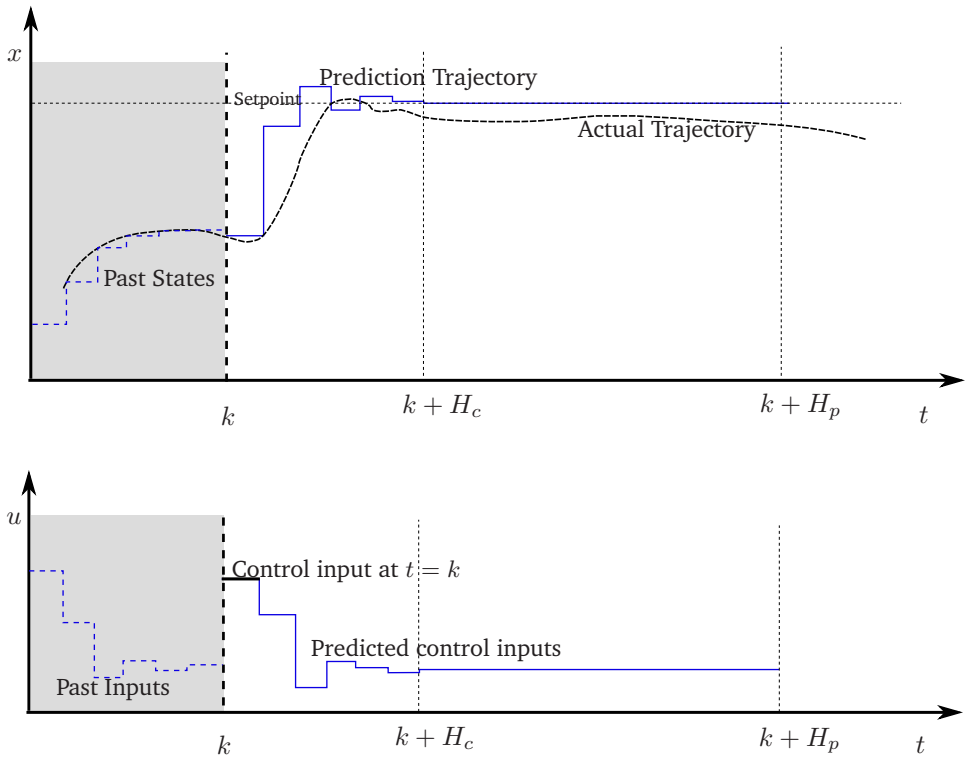

Figure 4.1: Illustration of the basic concept of predictive control. The top plot shows the developement of the system states, while the lower plot shows the control inputs.

$$J(u,k) = \sum_{i=1}^{H_p} (\bar{e}_{k+i}^{\top} Q \bar{e}_{k+i}) + \sum_{j=1}^{H_c} (u_{k+j}^{\top} R u_{k+j}) \tag{4.3}$$

where $\bar{e}_{k+i}$ is the predicted error at time step $k+i$ and Q and R are weighting matrices on the state error and the control action respectively. Depending on the application one can choose to punish a change in the control action Δu, rather than the magnitude of the control action, $|u|$. If the control input is e.g. to turn a valve, it would make sense to punish Δu to limit the wear in the actuator, while if the control input is fuel input it would make sense to limit the total fuel consumption, i.e. $|u|$. The reference values that are used to calculate $\bar{e_{k+i}}$ can change over the prediction horizon, if that is desirable.

MPC can handle constant disturbances and plant/model mismatch by estimating the prediction error defined as (Maciejowski (2002))

$$\epsilon_k = y_k - \bar{y}_{k|k-1} \tag{4.4}$$

where y_k is the measured state at time-step k and $\bar{y}_{k|k-1}$ is the predicted state for time k predicted at time $k-1$. If the output error is assumed to be integrated white noise - which is common - the best projected value for the future disturbance is

$$\epsilon_{k+i} = \epsilon_k \tag{4.5}$$

By including this estimate in the controller an offset-free response can be achieved in the presence of model-system-mismatch or a constant disturbance. This replaces the integral action used in conventional control.

One of the major advantages of MPC is the ability to handle constraints. This means that it is possible to set values for all states and all inputs that the plant should not cross at any time. This means that a predictive controller would react differently to a disturbance if this disturbance pushes the system towards a constraint, than if the disturbance pushes the states away from the same constraints. This is the main difference from a linear controller. In fact, when no constraints are active a predictive controller can often be reduced to a linear, multivariable controller.

MPC was originally developed for slow, stable plants in the process industry, were stability was not a problem. With the recent attention to use MPC also for faster and more dynamically complex systems, more attention has to be given to stability. An important factor for stability is that the prediction model is stable, and if the system is unstable this is obviously not the case. Maciejowski (2002) suggests replacing the A-matrix of (4.2) which is unstable with $A - B\,K$ in the predictions. K is a stabilizing feedback gain.

4.2.2 MPC Implementation

The wind turbine that is to be controlled is subject to a lot of constraints on both input variables and states. The pitch angle has a minimum angle to avoid stall, the generator has a maximum output power and the turbine speed should be kept below the maximum turning rate. It is also desirable to maximize the power output, and minimize undesired vibrations. These are all factors that give incentives to look into MPC as a control method for the floating wind turbine.

There are, however, some challenges related to this MPC application as well. The system is not stable, something that is shown in Section 3.4.1. That has to be taken care of. The system also have a large dynamic range. There are fast - and even unstable - dynamics in the drive-train, while the tilt frequency of the tower has very slow dynamics. The consequences of this will be discussed further in the later chapters. The system is also rather non-linear and this could yield difficult challenges.

As mentioned the *Model Predictive Control Toolbox* in Matlab is used to implement the MPC controller in Matlab and Simulink. The linear control model from section 3.3 is used and the step size is chosen to be smaller than the dynamics of the unstable dynamics of the drive train. The prediction horizon must be long enough to capture the dynamics of the tower.

The model developed in Section 3.3 is a contiious model, and the discrete model is obtained using the `c2d` function in Matlab.

The wind is modeled as an unmeasured disturbance with know frequency distribution. The frequency distribution is the transfer function from (3.37). Similarly the wavemodel is implemented, as in Section 3.2.8.

The controller is tuned by adjusting the weight matrices Q and R, and setting the constraints. The input power is constrained to its rated value, while the rotor speed is constrained 10% above the rated value[1]. The pitch angle is constrained at 0° and the pitch rate is constrained to $\pm 3^\circ/s$.

Deviations in the following states are weighted; generator side turbine speed, ω_e, drive shaft twist angle, θ, and the tilt speed, Θ.

[1] Why is the turbine speed not constrained to the rated value? That would make sense, but to the best of the authors understanding there exists an agreement in the industry that this is a *recommended* value, and that the turbine speed should not be *too much* higher than the rated value.

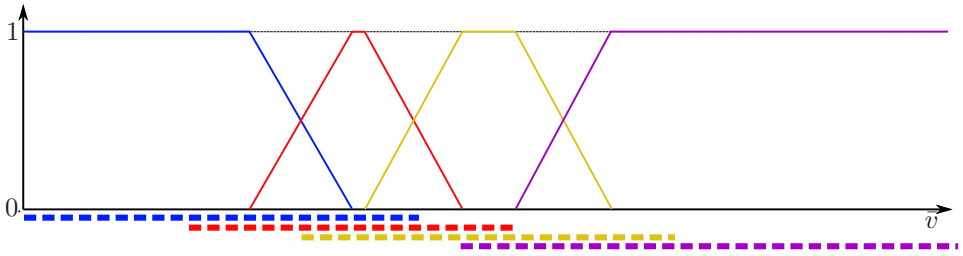

Figure 4.2: Illustration of the "fuzzy" controller selection scheme. Dotted lines indicate when the controller is running.

4.2.3 Global Solution/Bumpless Transfer

The simulation model is very nonlinear and this impedes the use of *one* linear model for the entire operation area. The solution to this challenge is to design several MPC controllers in four different operating points and with different desired functionality. Different operating points has a different control objective (See Sec. 4.1), and requires a different control strategy

Which controller that runs is decided from the wind estimate described in Section 3.2.7. The wind estimate decides the operating point, which in turn decides which controller is active. To achieve smooth transitions between operating points is called *bumpless transfer*.

Because the MPC algorithm uses past states and control inputs to estimate the system state and calculate the optimal future input sequence, the controller can not be "cold started" - i.e. it has to run and be aware of both the actual input and the measurements before it is made active. Even when the controller is running, a sudden transfer from one controller to the other is likely to cause an uneven system behaviour. To reduce this effect a fuzzy-like approach is made to switch between the controllers. This involves gradually changing between a controller and the next based on the wind estimate. This is illustrated in Figure 4.2.

With this solution the estimate of the wind is very important. If the controllers are very different the system becomes very sensitive to errors in the wind estimate. Thus it is advisable to have fairly robust controllers especcially around rated wind speed were the control objective can change much even for a small change in the operating point.

4.3 Alternative Controllers

In order to evaluate the performance of the developed MPC controller, it is necessarry to compare it to other solutions. In this section three different alternative controller is described, and two is implemented. A *Linear Quadratic controller* is developed by the author, while an *estimator based controller* and an *increment pitch angle controller* is based on patents from StatoilHydro and Sintef respectively.

4.3.1 LQ control

The MPC solution in the previous section could as mentioned be reduced to an LQ-controller without the constraints. Therefore it could be useful to compare the MPC solution to an LQ-controller to see if the constraints lead to better results or not. A gain-scheduled, linear, multi-variable state-feedback controller will be implemented. A block diagram of the controller can be found in Figure 4.3.

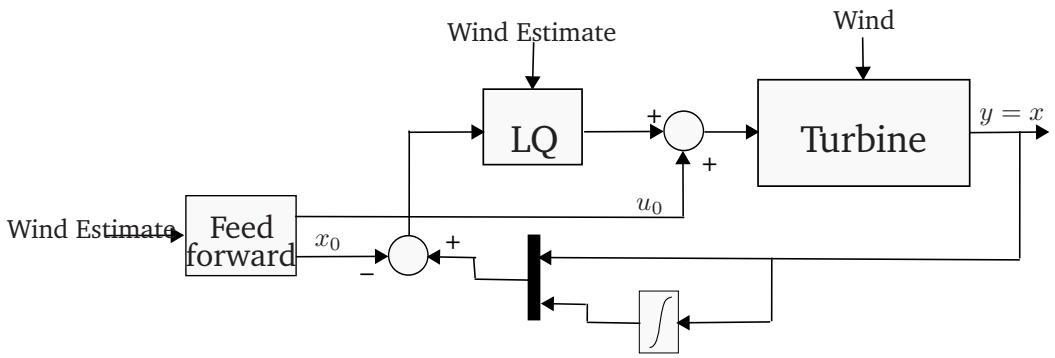

Figure 4.3: Block diagram of the LQ controller design

A prerequisite for use of LQ-control is that the full state is available, and this is assumed in Section 3.4.2. Section 3.4.1 also states that the system is controllable, but, as discussed in Section 3.4.3, even though the the blade edgewise flapping is theoretically controllable, it could be difficult to damp out the vibrations.

The state feedback controller will be applied to perturbations from the operating point. This means that the total control input will be composed of two parts:

$$\mathbf{u} = \mathbf{u}_0 + \Delta\mathbf{u} \tag{4.6}$$

where $\Delta\mathbf{u}$ is the output of the state feedback controller and is on the form

$$\Delta\mathbf{u} = -K\Delta\mathbf{x} \tag{4.7}$$

and is applied to the linearized system developed in Section 3.3 to yield

$$\Delta\dot{\mathbf{x}} = (A - BK)\Delta\mathbf{x} \tag{4.8}$$
$$\mathbf{y} = C\Delta\mathbf{x} \tag{4.9}$$

K is the optimal control gain that minimizes the cost function

$$J(u) = \int_0^t [x^\top Q x + u^\top R u]dt \tag{4.10}$$

where Q and R are diagonal weighting matrices.
The gain, K, of the optimal solution (4.7) is given by

$$K = R^{-1}B^\top X \tag{4.11}$$

X is the solution of the Riccati Equation

$$A^\top X + XA - XBR^{-1}B^\top X + Q = 0 \tag{4.12}$$

The LQ controller is evaluated for the linearized model developed in Section 3.3, and the gain, K, is calculated by the `lqr`-command in MatLab.

u_0 in (4.6) depends on the estimate of the wind speed, and this is represtented by the feed forward block in Figure 4.3. This solution is vulnerable to errors and fast changes in the wind estimate, and such errors could possibly yield suboptimal performance of the controller

Integral States for the LQ Controller

LQ control in its most basic form is basically a PD-controller, and it does not have any integral action. The MPC-algorithm overcomes this by estimating the error, but this solution will use a more classic approach. E.g. Skogestad & Postletwaite (2005) suggests adding additional integral states to the model. Our main goal is to keep the turbine speed and the output power close to the desired values and therefore we add two integral states

$$\omega_{int} = \int_0^t \omega_{ref} - \omega_t \, dt \tag{4.13}$$

$$P_{int} = \int_0^t P_{ref} - P \, dt \tag{4.14}$$

By realizing that the linearized system has no reference input and differentiation of (4.13), (4.14) yields the two new states to be added to the linear state space solution

$$\dot{\omega}_{int} = -\omega_t \tag{4.15}$$

$$\dot{P}_{int} = -P \tag{4.16}$$

Gain Scheduling

In order to handle the nonlinearities in the system the LQ controller is evaluated in several equilibrium points of the system for different operating conditions. The operating point and hence the feedback gain is decided based on the current estimate of the effective wind speed. The expression for this was given in (3.43). The actual K-matrix is an interpolation of the calculated K matrices of the two closest operating points. This is also true for the operating points $(\mathbf{x}_0, \mathbf{u}_0)$ themselves. This strategy is similar, but not identical to the bumpless transfer algorithm from Section 4.2.3.

The weighting matrices of the LQR algorithm are the design parameters of the LQ controller, and these are varied according to the operating condition. For wind speeds above rated the most important goal is to keep the output power close to the rated value. The use of pitch and, to a certain extent, variations in the turbine speed are not that important. For low wind speeds maximum efficiency is the most important thing. Here the weighting matrices are chosen to keep the pitch angle close to the optimum, (β_0), and to keep the turbine speed close to the optimal value.

Stability

Gain-Scheduled controllers are somewhat difficult to handle when it comes to stability. The literature gives little help in proving stability and in fact it, e.g. in Slotine & Li (1991), states that it can not be proven. Stability can be shown in each of the operating points, and the total system is stable as long as the gains are not adjusted *too fast*. How fast *too fast* is, is however hard to establish.

The individual controllers in each of the operating points have better stability properties. By assuming that all states are available for measurement and choosing diagonal weighting matrices Q and R (4.10) Safonov & Athans (1977) states that we will have a 60° phase margin, a lower gain margin of 0.5 and a gain margin of ∞.

The eigenvalues of $(A-BK)$ have all negative real parts for all operating points.

The main source of error and the biggest risk for stability problems will be related to the estimation of the effective wind speed. Deviations in the measurements, the assumed Cp-value or other problems might lead to wrong estimates that

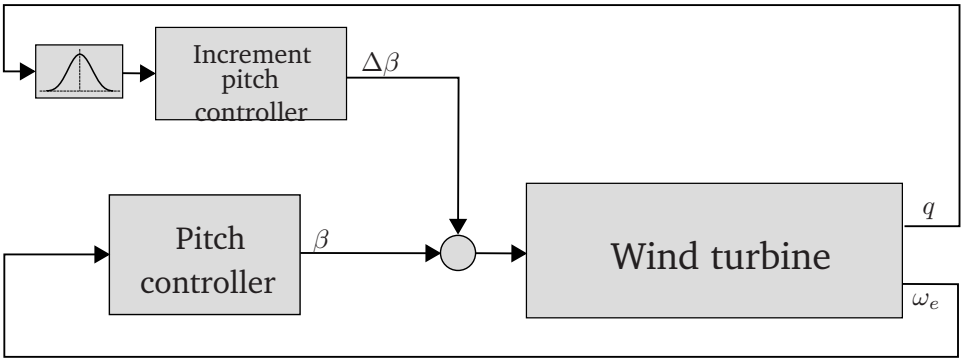

Figure 4.4: Sketch of the controller structure for the increment pitch angle controller.

in closed loop might lead to unwanted dynamic effects. Even with a good estimate using a Kalman Estimator stability cannot be proven. LQ control combined with a Kalman filter yields what is known as LQG control and its stability margins was famously discredited in Doyle (1978).

4.3.2 Increment Pitch Angle Controller

In the initial phase of the Hywind project a controller with an increment pitch angle controller was proposed. This solution was developed in connection with the model testing by Sintef and Marintek (SintefEnergyResearch (2005)), and a patent on the solution was granted in 2008 (Nielsen et al. (2008)).

The solution involves a regular pitch angle controller that is augmented by an increment pitch angle controller. The increment controller measures the tilting speed of the turbine, filter out the oscillating frequency of the tower, and gives a pitch angle signal out that aims to limit the unwanted positive feedback from the tower motion. A sketch of the controller structure is shown in Figure 4.4.

If the tower moves up-wind the regular pitch controller would increase the blade pitch angle to account for the increased effective wind velocity induced by the tower movement. In this situation the increment pitch controller would give a *negative* increment pitch signal, to avoid the increase in the drag force that the increased pitch angle would have led to.

The increment controller is designed to counteract the regular pitch controller at the eigen-frequency of the tower, and allow the turbine speed to vary with this frequency. It is therefore necessary that the pitch controller is not too fast. If for example a PI-controller is used and this is too fast it would "chase" the damping controller, and cancel its effect.

The output power is decided as described in Section 2.2.2. Because this controller has to be rather slow, large fluctuations in output power can be expected, and this requires that the output power is kept at the rated value below the nominal turbine speed. The output power is equal to 1 for turbine speeds above 0.9 times the nominal speed.

4.3.3 Estimator Based Controller

A recent patent (Skaare (2009)) by StatoilHydro suggest a different approach to the part of the control problem that involves damping of the tower vibrations. See Section 3.4.4 for details on this problem. The basic idea is to use an estimate of the actual wind velocity - excluding the tower movement - to estimate what the turbine

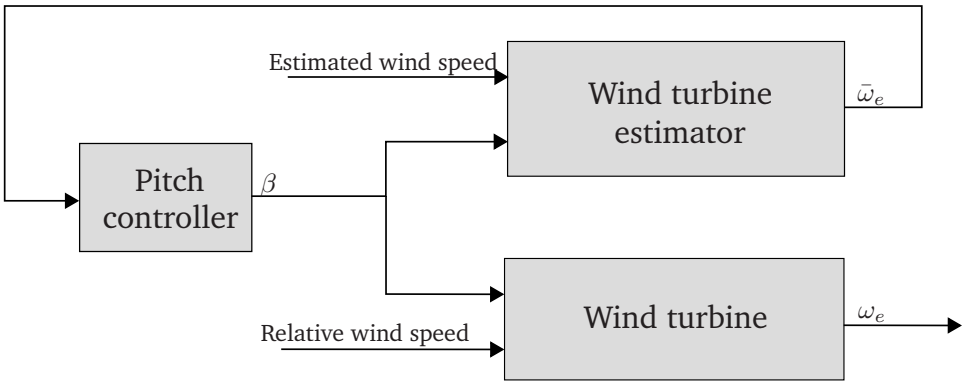

Figure 4.5: Sketch of the suggested estimator based controller. Figure reproduced from Skaare (2009).

speed would have been was it not for the motions induced by the tower movement. The procedure is illustrated in Figure 4.5.

By estimating the wind turbine speed resulting from the estimated wind velocity, the changes in turbine speed resulting from the tower tilt motion is "hidden" from the pitch controller. By doing this the positive feedback problem is avoided.

An advantage with this solution is that it is easy to mix with a factory made pitch controller. A key element in the Hywind project is the ability to use an of-the-shelf wind turbine, and mount it on a floating platform. This control solution also allows the use of the factory-made pitch controller, the only adjustment is to exchange the measured wind turbine speed with the estimated. A possible, but not substantial, drawback with the solution is that it could be difficult to obtain a reliable estimate of the wind speed. Also, no additional damping of the tower movement is introduced.

This patented solution was not published until May 2009, and has not been implemented in this paper. Comparing the results from this report with the patented solution is left for future research.

Chapter 5

Simulations

5.1 Verification of the linear model

The linearized model presented in Section 3.3 is essential for the controller design of the LQ- and the MPC controllers. Therefore it is important to see if the linear model represent the dynamics of the system properly. Figure 5.1 shows a comparison of the linear and the nonlinear model. The systems are controlled with a simple PID controller, and it can be seen that they show similar, altough not identical responses. The oscillation frequencies seem to be almost identical and that is the most important for good prediction.

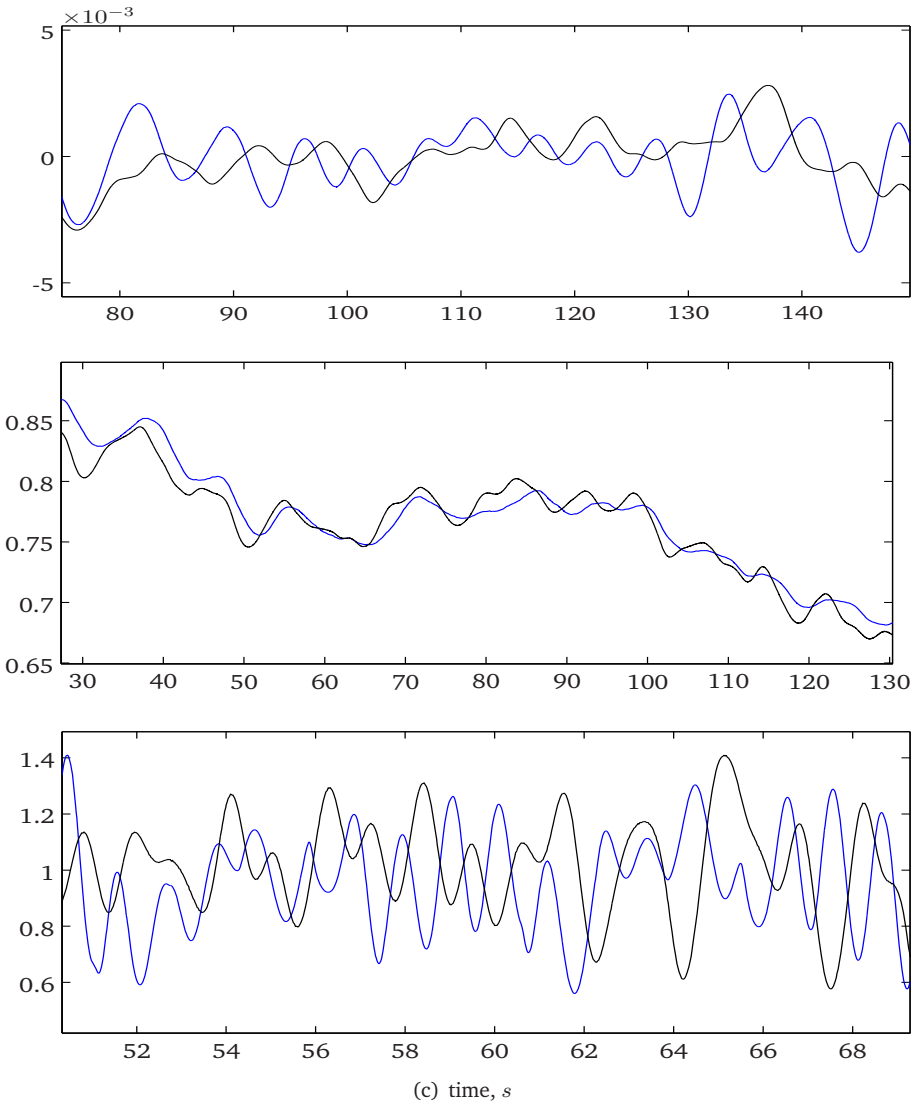

Figure 5.1: Comparison of the linearized(black) and nonlinear(blue) models. Top: Tower tilt motion (rad/s); Middle: Turbine speed (pu); Bottom: Blade vibrations(pu)

5.2 Model Predictive Control

The wind model predicts the future wind disturbance. Figure 5.2 shows the predicted wind disturbance at a controller timestep for each of the blades. We can see that it fluctuates with a frequency around the turbine rotational frequency ($12.1\,rpm \approx 1.2\,rad/s$), and that the fluctuations are roughly $2\pi/3\,rad$ out of phase for the three blades.

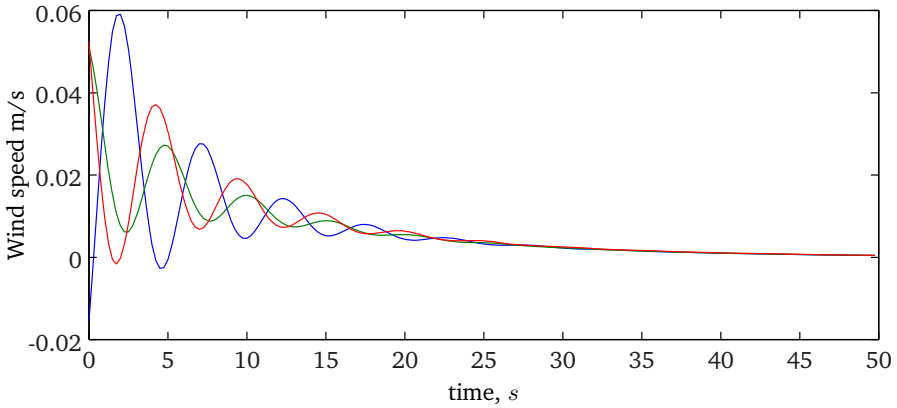

Figure 5.2: Predicted wind values for the estimated wind

5.2.1 Adjusting the parameters

In the design of the MPC there are many parameters that have influence on the performance of the controller. These parameters include the control horizon, the prediction horizon, the time step length and of course the weights on the states. To show the effect of all these parameters would be too expansive, but some will be presented below.

The dynamic range of the system is large. In order to have control of the faster dynamics, the time-step must be short enough, while the prediction horizon must be long enough to capture the slower dynamics of the tower movement. Figure 5.3(a) show the effect on tower movement from changing the prediction horizon and the effect of drive train damping from changing the time step. This demonstrates the claims made that the prediction horizon should be long, and the time step short.

The *wave model* from Section 3.2.8 is included, but the simulations do not indicate that this is decisive for the performance of the system. Figure 5.4 shows that the tilt movement is almost identical, but that the turbine speed control is slightly better. This might be because the controller with the wave model predicts the future movement of the tower better, but it is difficult to be conclusive.

A goal of this project was to be able to reduce edgewise vibrations in the blades. Therefore it was natural to try to add weight on the blade angle so that the MPC would damp out these vibrations. However, Figure 5.5 (a) shows that this is counterproductive, and that the controller is not able to reduce the blade vibrations more by adding weight to the states. Figure 5.5 (b) and (c) shows that the controller is using the pitch output more, trying to control the vibrations. The three pitch signals are out of phase with each other as expected, but without giving the desired effect. The frequency of the pitch input signal is around the rotational frequency, and this might be because the controller, predicts the periodic fluctuations in wind speed as in Fig. 5.2 and tries to control the pitch accordingly.

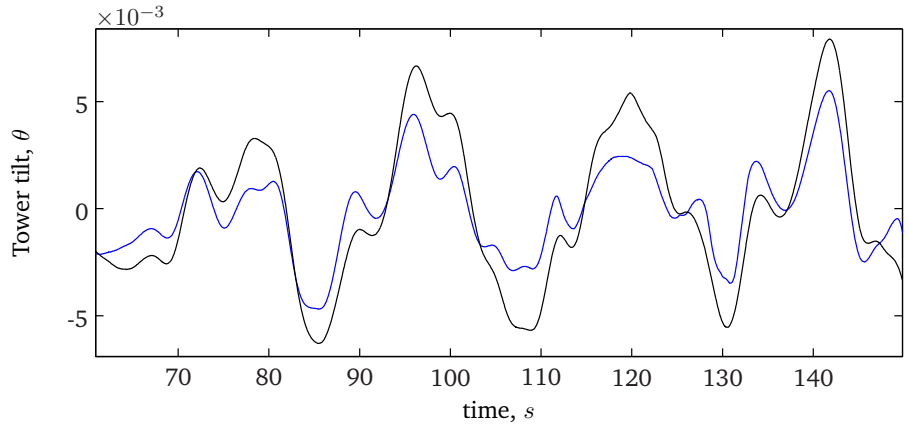

(a) Tilt movement. $H_p = 200$(blue) and $H_p = 75$ (black)

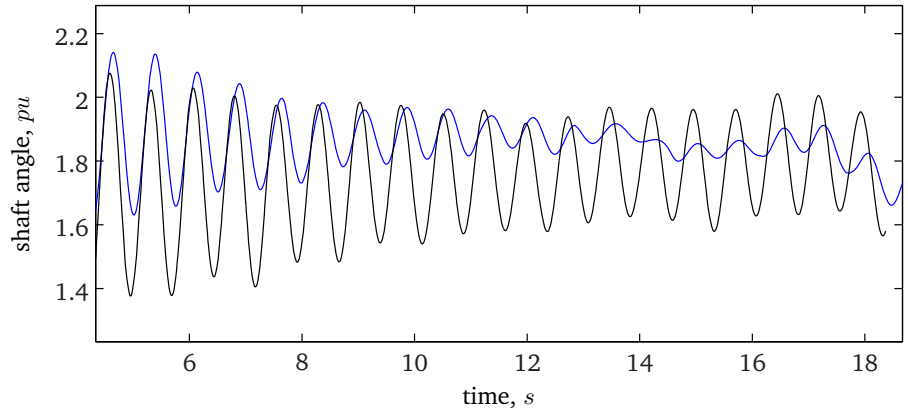

(b) Drive train oscillations. Time step $0.25s$(blue) and $0.5s$(black)

Figure 5.3: Tilt motion of the turbine with different prediction horizons (a) and drive train oscilllations for different time steps (b)

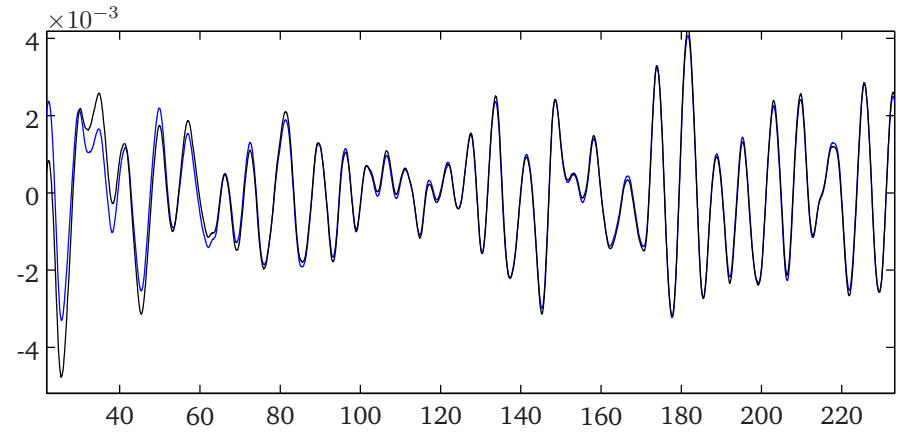

(a) Tilt movement. With wavemodel(black) and without(blue)

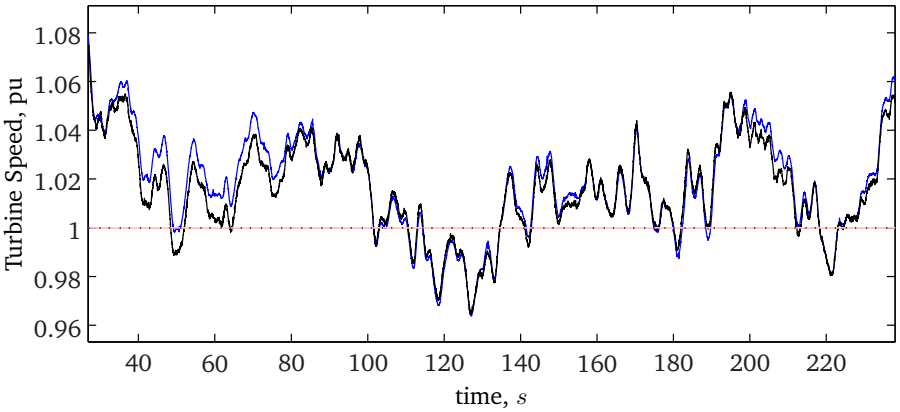

(b) Turbine speed with wavemodel(black) and without(blue)

Figure 5.4: Effect of including the wave model. Tilt motion ((a)) and turbine speed ((b))

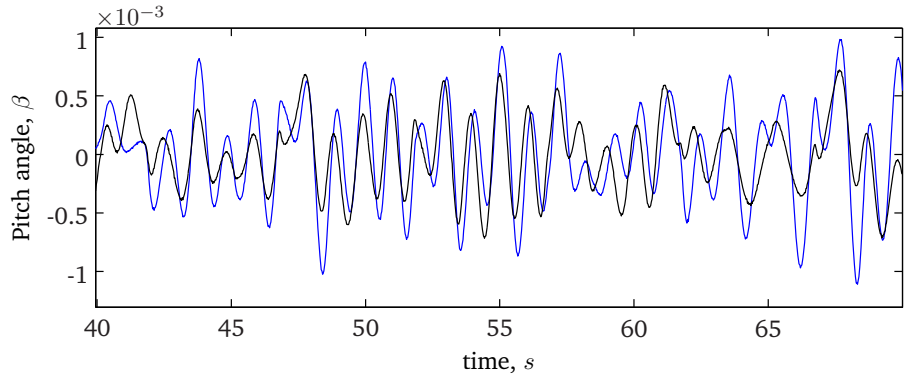

(a) High-pass filtered measurement of blade vibrations with(blue) and without(black) weight on the blade angle

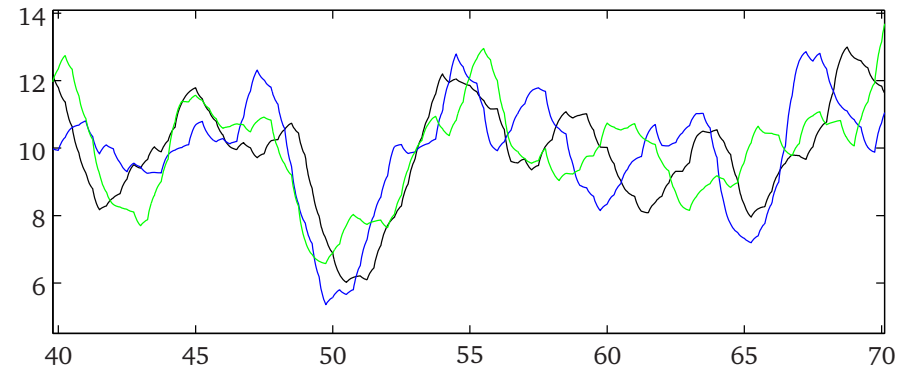

(b) Pitch angle of the blades when the blade bending is weighed

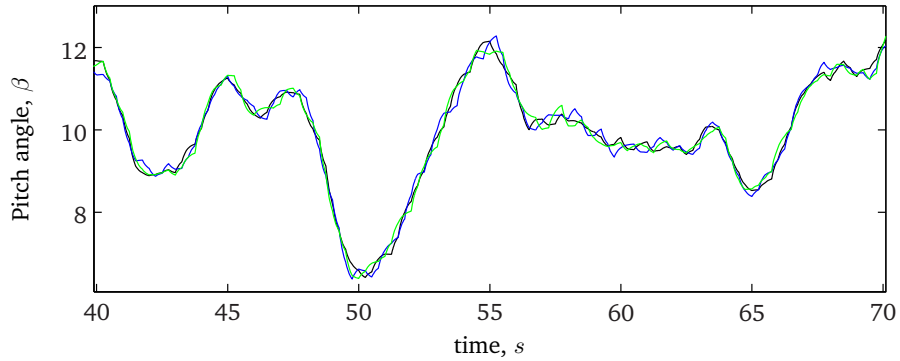

(c) Pitch angle of the blades when the blade bending is not weighed

Figure 5.5: Effect of adding weight on the blade edge-wise bending. (a) blade edge-wise fluctuations; (b) Pitch actuation when punishing blade bending; (c)) Pitch actuation when not weighing the blade bending.

5.2.2 Bumpless transfer

The MPC solution is designed to work for all wind speeds, and this is done by switching between controllers tuned for different operating ranges. This is done by gradually changing the input from the different controllers based on a "fuzzy-like" switching regime as described in Section 4.2.3.

In order to test the bumpless transfer design it is simulated with a gradually increasing and decreasing wind speed. The wind starts at $\approx 6m/s$ and increases to $\approx 16m/s$ in about 5 min, before decreasing to $\approx 6m/s$ again. The waveheight for these simulations are $3m$, and the turbulence intensity is 15%

The results are shown in Figure 5.6. In the fourth subplot we can see when the different controllers are active. The sum of all the controller weights or factors are always equal to one.

The lowest plot shows the average wind speed, and the estimated wind speed, and it can be seen that the estimate is good. This is important because the controller switching algorithm uses the estimated wind speed as input.

From the top three plots in Figure 5.6 we can see that the performance of the controller is not compromized when changing between the controllers. The turbine speed tracking is acceptable and so is the damping of the tower oscillations.

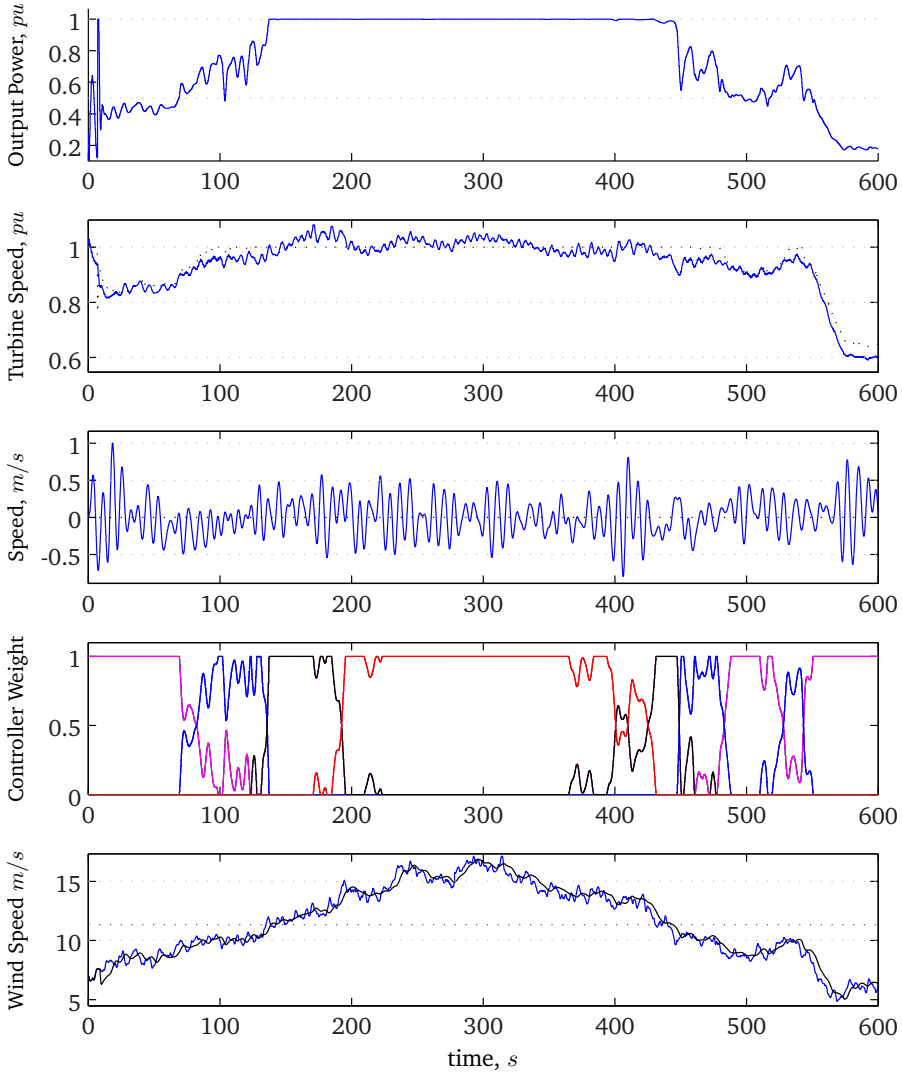

Figure 5.6: Simulation of the MPC controlled wind turbine for rising and increasing winds. From the top: 1: Output power; 2: Turbine speed; 3: Nacelle movement, induced motion of the nacelle into the wind; 4: Controller Selection, different controllers tuned for different wind speeds, (from lower to higher - magenta, blue, black, red); 5: Average wind speed(blue) and estimated wind speed(black)

5.3 Comparison of Controllers

Three different controllers were implemented in Section 4.3. The controllers are very different in style and complexity but still the following will try to evaluate their performance and compare them.

The three controllers are tested in simulation for three different operating regimes: Weaker winds around $8m/s$, winds around the rated value at $11.5m/s$ and in strong winds around $16m/s$ in the power limitation regime. These values should give good insight in in the performance of the controllers in the power optimization range, when changing between power maximization and limitation and in the power limitation range respectively. The average wave height is also varied and follows the mean wind speed according to the Beaufort scale (Fossen (2002)). In order to test the controllers the turbulence intensity is chosen to be rather large, 15%.

Table 5.1 shows some key simulation results for the three simulations and Figures 5.7 - 5.9 show more detailed plots of the simulations.

Figure 5.7 shows the performance of the system for low wind speeds. It can be seen that the MPC gives smooth power output, but has a small steady state offset in the turbine speed; it does not follow the desired value entirely. The top plot shows that the PID controller gives some spikes in the output power. This is due to the power setpoint calculation presented in Section 2.2.2. The reduction of the tower movement, and the blade bending movements are not substantially different.

Figure 5.8 shows simulations in wind strength around rated speed. This is the most difficult operating range to control because of the chancing control objective at rated wind speed from power maximization to power limitation. Also this is the area where the drag forces are strongest (see Fig. 3.14). Here, it can be seen that the LQ controller performs poorly. The LQ controller is dependant on a good estimate of the wind speed. When simulating the system with turbulent winds we can see that this estimate is not good enough and that it gives large transients. The PID controller shows large overshoots in turbine speed, but performs otherwise satisfactory. The MPC controller is working well, and the switching algorithm presented in Sec. 4.2.3 is working superbly. Again, the reduction of tower movement is comparable, while it is interesting to see that the blade bending is better damped out for the LQ controller, and that it uses the pitch input less. This might indicate that the LQ controller is not tuned exactly like the other controllers, and that extensive pitch control might increase blade vibrations.

The system response in the power limitation area can be seen in Figure 5.9. Here the LQ controller and the MPC controller perform similarly, with rather tight control of the turbine speed and almost steady output power (the MPC controller is strictly constrained to give rated power so it does not vary at all). From Table 5.1 it can be seen that the MPC controller damps out the tower movement slightly more than the others, and that the blade bending is less intense than for the two other controllers. Again the LQ controllers uses the pitch actuators less intensively than the other controllers. The PID controller is not able to limit the tower movement as well as the other controllers, and large fluctuations in the turbine speed leads to unnecessary drops in the output power.

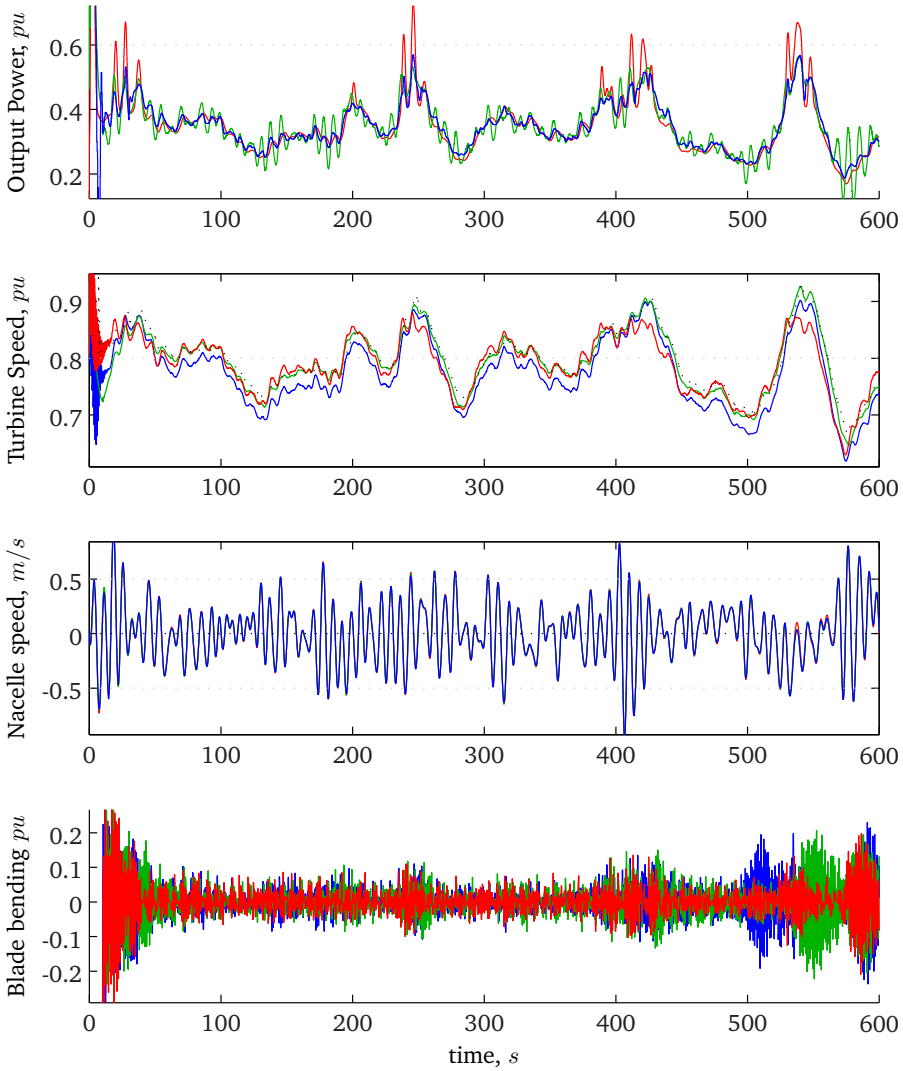

Figure 5.7: Simulation of the wind turbine. $\bar{v} = 8m/s$, avg. wave height is $2m$, $I_{trb} = 0.15$. PID controller(red), LQ controller(green) and MPC controller (blue)

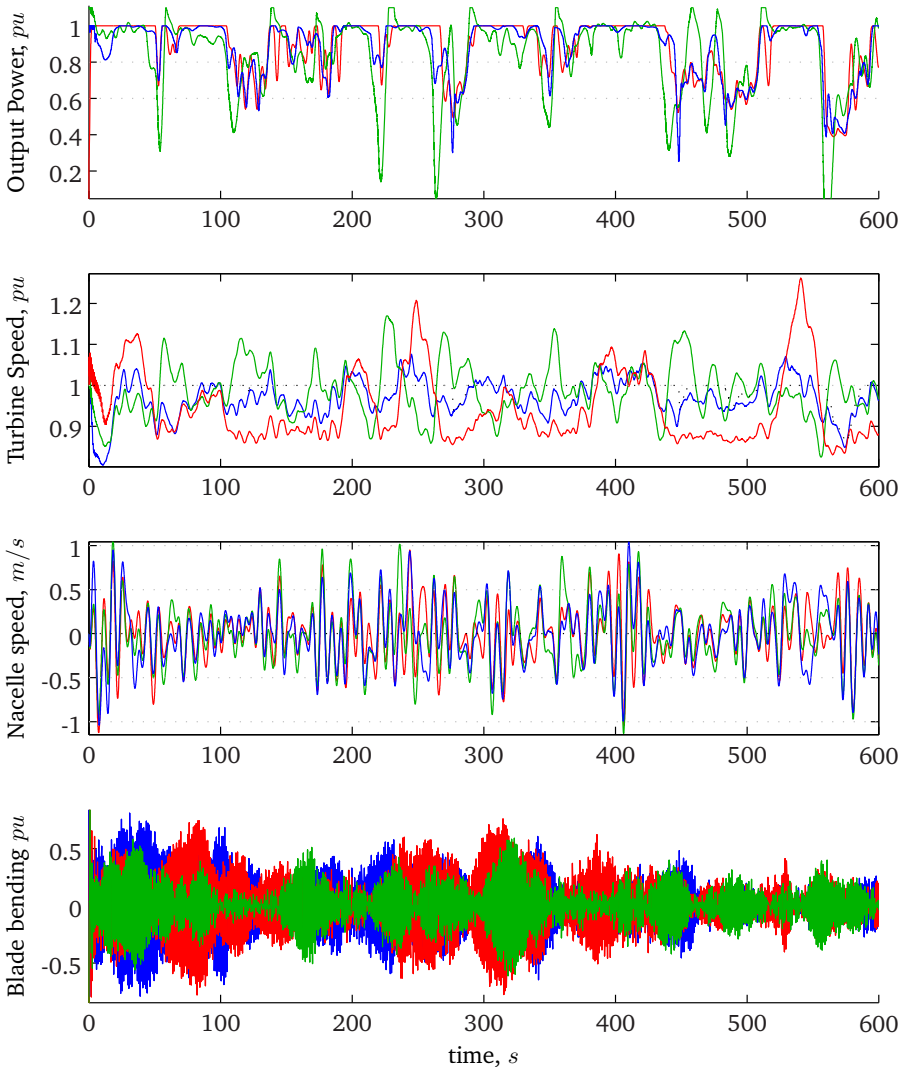

Figure 5.8: Simulation of the wind turbine. $\bar{v} = 12m/s$, avg. wave height is $3m$, $I_{trb} = 0.15$. PID controller(red), LQ controller(green) and MPC controller (blue)

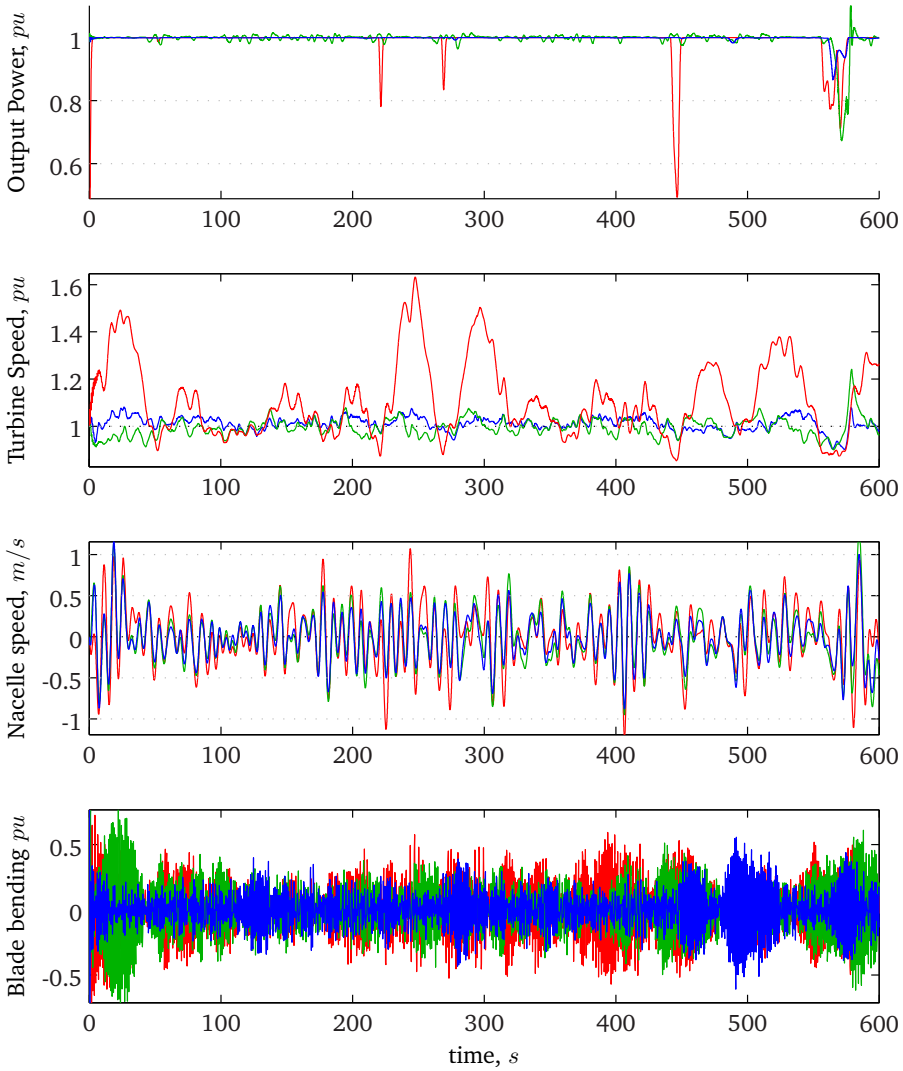

Figure 5.9: Simulation of the wind turbine. $\bar{v} = 16m/s$, avg. wave height is $5m$, $I_{trb} = 0.15$. PID controller(red), LQ controller(green) and MPC controller(blue)

$8m/s$	Produced power, pu	RMS tilt, m/s	RMS blade, $10^{-3}rad$	avg $\dot{\beta}$
PID	212	0.21	34.6	≈ 0
LQ	212	0.21	41.7	≈ 0
MPC	212	0.21	39.6	≈ 0
$12m/s$				
PID	530	0.24	206	.56
LQ	505	0.27	142	.43
MPC	527	0.26	194	.56
$16m/s$				
PID	593	0.28	170	.94
LQ	597	0.24	157	.55
MPC	599	0.22	116	.92

Table 5.1: Table of key figures from the simulations

Chapter 6

Discussion

The goal of this project was to implement a unified control structure for the control and load mitigation of a floating offshore wind turbine. Because of the constraints in the system on pitch angle and maximum generator power, it was decided to implement a Model Predictive Controller to control the system. For comparison a modified PID controller and an LQ-controller was also developed. In Chapter 5 various simulations were performed in order to assess the performance of the controllers and the importance of the different parameters.

6.1 The Model

A large part of this project has been devoted to making a simulator of the wind turbine in Simulink and MatLab. The common approach of modeling the drive train as two masses connected with a flexible shaft is augmented to also include the edge-wise blade bending. This is, to the best of the authors knowledge, a novel approach to this modeling challenge and this seems to work well. For control purposes, it might be a good modeling strategy also for future projects. In relation to this it should be noted that the structural dynamics of a wind turbine blade are very complex. Higher frequency modes are present and it probably exist more coupling between the pitch movement and the blade dynamics than is modeled here. However, the two degrees of freedom that are modeled here can arguably be said to be the two most important, and also the two that are most likely to be affected by control.

The turbine model is based on data from the NREL reference wind turbine for offshore applications. This model is the de-facto industry standard for wind turbine modeling and this data should thus be reliable. The floating tower model is created with state-of-the art modeling software, and can also be expected to give a realistic model.

The model has not been tested with experimental data. Still, the independent parts of the model are based on well known modeling approaches and renowned turbine data. Thus the results should not be too unrealistic. Most uncertainty is related to the blade modeling.

6.2 The MPC Controller

The MPC controller aimed to control the turbine for the whole operating range, and at the same time reduce the vibrations in the blades and avoid exciting the tower

eigenfrequency. The simulation results indicate good goal achievement for parts of this ambition, while the effect is less apparent on other aspects.

The main strong points of the MPC solution is the good global operation. The simulations in Section 5.2.2 shows that the controller works well for the whole operating range, and handles the transition between wind speeds below and above rated wind speed very well. The MPC controller also manages to have good control of the turbine speed, while still avoiding the problem with positive feedback from the tower movement as described in Section 3.4.4. The possibility of constraining the output power to the rated value also gives very smooth output power when in the power limitation operating range.

The MPC controller also aimed at reducing the edge-wise blade vibrations, and this required increased complexity of the controller, with a more complex model and more (assumed) measurements. However, it is not possible at this point to conclude that this effort has been very successful. No significant improvement over the simpler controllers are seen and, as shown in Figure 5.5, adding weight on the coherent states actually proved to be counterproductive.

Still it is fair to say the overall operation of the controller is good, and that the results show that MPC could be a good alternative when designing controllers for offshore wind turbines.

6.3 Comparison of the Controllers

In Section 5.3 the three developed controllers were tested in the same wind conditions.

The controllers performed similarly for the low wind speed case (Fig. 5.7). The MPC controller did not achieve perfect tracking of the turbine speed reference, while the power set point calculation for the PID controller leads to som sharp peaks in output power for turbine speed above 0.85% of the nominal speed.

The differences are more apparent around the rated wind speed, as can be seen in Figure 5.8. The switching algorithm for the LQ-controller design is not working as it should around rated wind speed. This problem arise because the LQ-controller depends on a good estimate of the current wind speed, and this is not achieved here. It is worth mentioning that this is a problem with *this implementation* of the LQ controller, not LQ control itself. An LQ controller implemented with a switching regime like that of the MPC controller could probably work better. The MPC controller works well, while the PID solution gives larger overshoots in the turbine speed. The increment pitch control for the PID works well and damps out the tilt motion slightly better than the MPC controller.

The response to strong winds can be seen in Figure 5.9. It shows that the LQ controller and the MPC controller works similarly, while the PID controller is not performing well at all. The increment pitch controller leads to large variations in the turbine speed, and this again leads to unnecessary drops in the output power. The LQ and MPC controllers damp out the tower motions better while at the same time keeping the variations in turbine speed at an acceptable level. It is interesting to note that the variations in turbine speed has the same period as the eigenvalue of the tower motion ($\approx 40s$). Increasing the turbine speed slightly when moving into the wind and reducing it when moving out of the wind. This is the same response as the two patented solutions presented in Section 4.3 aims for, and shows that the MPC solves this problem well.

It is not possible to conclude one way or another with regards to the edge-wise blade vibration. Table 5.1 shows the mean value of the deflection for the different controllers and scenarios, and there are no clear patterns as to which controller

performs best. The fact that each controller "wins" one scenario, makes it easy to conclude that it is difficult to conclude.

6.4 Other Remarks

It is important to be aware that the controllers work with entirely different information of the system. The PID controller measures only the turbine speed at each end of the drive train and the nacelle movement, while the other two controllers require measurements (or good estimates) of all states including blade edgewise bending, and they also use explicit knowledge of the model dynamics. Thus it is necessary to evaluate if the performance gains can justify the increased complexity in the control system. The increasing size and cost of the individual wind turbines will presumably lead to more advanced measurement equipment and control systems. This could make it possible to use more advanced control methods, and more measurements in the future wind turbine control systems, even with the relatively small performance gains that are seen here. One wind turbine is rarely very different from the next, and this makes it possible to develop advanced controllers that can be installed in many turbines.

All the controllers that have been developed in this thesis are designed to work for the entire operating range of the turbine. Today, most commercial wind turbine control designs have different designs for different operating regimes. It could be argued that there is not a lot to gain by making one global controller. The big fluctuations in wind speed are slow, and related to weather changes, therefore it is possible to imagine having completely different controllers for different conditions. One controller could be designed to give perfect tracking of the optimal tip speed ratio in weak winds, and in strong winds another one could focus solely on the power limitation. The implemented MPC solution is indeed made of four different controllers, but it could be possible to exchange some of these with other controller types. The "fuzzy" switching algorithm performes very well and could possibly be used also when the controllers are of different types. The PID controller, for instance, performed better than the MPC controller in the low wind speed scenario in the simulations above. Then this could have been used in that range, while the MPC could be used in the other operating regimes.

Better solutions for load mitigation in the blades should be possible to develop. Many of the proposed solutions use some sort of cyclic approach and decouples the load mitigation control problem from the power limitation control problem. This thesis wanted to explore if a unified approach could be used, but no positive conclusion can be made.

6.5 Further Work

Include Flap To include the flapping equations in the MPC controller is an obvious addition to this work. The flapping motion is actuated by many of the same periodic drag variations as the edgewise vibrations, and the inclusion of this should not be too much work.

Trimmed MPC Solution As mentioned above the advantages of the MPC solution are most apparent for the tower tilt motion reduction and standard power control. Thus, implementation of a more limited MPC solution might yield even better results. This would mean using a model without individual blades and blade flapping.

Measurement and Estimation In this project good measurements of all states have been assumed, also of blade bending and the constructed blade rotational speed states. To avoid having to make assumptions like this a good estimator of the turbine and the turbine states would be necessary. A good estimator would also allow the use of techniques such as the estimator-based control design presented, but not implemented, in Section 4.3.3. Using an estimator to filter out wave-induced motions is a common strategy in marine control systems, and could be an attractive idea for this application too.

Fatigue Analysis of the Components In order to make a control system it is crucial to know what the control objective is. For a wind turbine control system that aims to increase the fatigue life of the total system it could be interesting to have a deeper insight in what parts of the wind turbine system that is most vulnerable to vibrations etc. How large oscillations are the different mechanical parts designed for? How much can the pitch control be used before the pitch actuators themselves become the weakest link? Is a turbine speed of 1.2 times the nominal value critical for the fatigue life of the turbine, or does it not really matter? This could be the subject of a more extensive literature survey, or a thesis in e.g. mechanical engineering. Such information should in turn be used to reformulate the control objective in detail for the wind turbine.

Start-up, Shut-down and Faults This thesis has looked at normal operation of the wind turbine. There are a number of challenges related to wind turbine control in other operating modes such as start-up, and shut down. In very strong winds (above $25m/s$) most wind turbines shut down and this, as well as starting back up when the wind speed decreases again, is a challenging task with room for further research and development.

Chapter 7

Conclusion

In this thesis a simulator for a floating offshore wind turbine has been successfully developed. It includes a model of the floating platform made with a state-of-the-art modeling program from the maritime industry as well as a novel approach to modeling of the in-plane blade vibrations. The model also include periodic effects such as wind shear and power shadow that are important when trying to understand the fatigue loads on a wind turbine. The simulator is presented in Section 3.2.

In Chapter 4 a Model Predictive Controller(MPC) has been implemented and the simulations in Chapter 5 shows that it works very well. The potential problem with negative damping of the tower movement that was described in Section 3.4.4 is handled convincingly.

The controller also aimed at reducing the edgewise blade vibrations, but this was not successful. In fact, the simulations presented in Figure 5.5 shows that trying to reduce the blade vibrations was actually counterproductive.

For comparison, two other controllers were designed; A PID controller was augmented with a patented increment pitch solution (Sec. 4.3.2) to handle the tower oscillation problem. It performed well for some scenarios but did not work satisfactory in strong winds. In Section 4.3.1 an LQ controller was implemented. This worked ok in strong winds but the implementation was not robust to errors in the wind estimation and this compromised its performance.

The switching algorithm presented in Section 4.2.3 that was used to switch between MPC controllers tuned for different operating ranges performed well, and gave smooth transitions when the wind increased or decreased around the rated wind speed.

The main contribution from this thesis is that it shows that Model Predictive Control can be successfully implemented on an floating offshore wind turbine and naturally cope with the issue of positive feedback from the tower movement.

In addition to this, the five-mass approach to the transmission and blade modeling provides an intuitive understanding of the interaction between the generator torque and the blade dynamics.

The "fuzzy" switching algorithm that was designed for the MPC could also be useful for other wind turbine control systems.

Appendix A

Linearization

The MatLab script for making the linear state-space system is repaeted below.

```
%-------------------------------------------------------------
%A-matrix
%-------------------------------------------------------------
%x = [w_t w_e \theta \beta1 \beta2 \beta3 ...
%     \xi_1 \xi_2 \xi_3 w_xi_1 w_xi_2 w_xi3 \eta \nu]'
Amat = zeros(18,18);

%wtDot
Amat(1,1)  = -Ddt/(2*Ht);
Amat(1,2)  = Ddt/(2*Ht);
Amat(1,3)  = -Ks/(2*Ht);
Amat(1,7)  = K_xi/(2*Ht*Pn*(1-esqrt2));
Amat(1,8)  = K_xi/(2*Ht*Pn*(1-esqrt2));
Amat(1,9)  = K_xi/(2*Ht*Pn*(1-esqrt2));

%wsDot
Amat(2,1) = Ddt/(2*Hs);
Amat(2,2) = 1/(2*Hs)*(Pset0/(ws0^2)-Ddt);
Amat(2,3) = Ks/(2*Hs);

%thetaDot
Amat(3,1) = 1*wn;
Amat(3,2) = -1*wn;

%beta
Amat(4,4) = -5;
Amat(5,5) = -5;
Amat(6,6) = -5;

%xidot
Amat(7:9, 10:12)=eye(3)*xiScale;
Amat(7:9, 1)=[-1;-1;-1]*xiScale;

%w_xi1_ddot
KVV = 1/wt0*(1-esqrt2)^2/6/I_blade*A*ro*vr0^3;
KV2 = 1/wt0*(1-esqrt2)^2/6/I_blade*A*ro*cp0*3*vr0^2;
KV3 = -1/wt0^2*(1-esqrt2)^2/6/I_blade*A*ro*cp0*vr0^3;
```

```
%wxi1
Amat(10,1) = D_blade_edge*(1-esqrt2)/I_blade;%KVV*dCPwt;
Amat(10,4) = KVV*dCPbeta; %Dxi/dBeta1
Amat(10,7) = -K_xi*(1-esqrt2)/I_blade; %dxi/dxi
Amat(10,10)= KVV * dCPxi + KV3 - D_blade_edge*(1-esqrt2)/I_blade; %dwxi/dwxi
Amat(10,16)= KVV * dCPv + KV2; %dxi/dsurge
Amat(10,18)= -KVV * dCPv*h - KV2*h; %dxi/dtilt

%wxi2
Amat(11,1) = D_blade_edge*(1-esqrt2)/I_blade;%KVV*dCPwt;
Amat(11,5) = KVV*dCPbeta; %Dxi/dBeta1
Amat(11,8) = -K_xi*(1-esqrt2)/I_blade; %dxi/dxi
Amat(11,11)= KVV * dCPxi + KV3 - D_blade_edge*(1-esqrt2)/I_blade; %dwxi/dwxi
Amat(11,16)= KVV * dCPv + KV2; %dxi/dsurge
Amat(11,18)= -KVV * dCPv*h - KV2*h; %dxi/dtilt

%wxi3
Amat(12,1) = D_blade_edge*(1-esqrt2)/I_blade;%KVV*dCPwt;
Amat(12,6) = KVV*dCPbeta; %Dxi/dBeta1
Amat(12,9) = -K_xi*(1-esqrt2)/I_blade; %dxi/dxi
Amat(12,12)= KVV * dCPxi + KV3 - D_blade_edge*(1-esqrt2)/I_blade; %dwxi/dwxi
Amat(12,16)= KVV * dCPv + KV2; %dxi/dsurge
Amat(12,18)= -KVV * dCPv*h - KV2*h; %dxi/dtilt

%eta
Amat(13:15, 16:18)=eye(3);

%nu
Amat(16:18, 13:15)= -MredInv*Dred;
Amat(16:18, 16:18)= -MredInv*Gred;

%-------------------------------------------------
%adding torque to Amat(16:18) - ddot(eta) -dot(nu)
KVT = 1/2*A*ro*(dCTv*vr0^2 + ct0*2*vr0) ;

Tmat = zeros(3,18);

Tmat(1,1) =  0; %KT*dCTwt;
Tmat(1,4) = - 1/6*A*ro*dCTbeta*vr0^2; %KT/3*dCTbeta;
Tmat(1,5) = - 1/6*A*ro*dCTbeta*vr0^2;
Tmat(1,6) = - 1/6*A*ro*dCTbeta*vr0^2;
Tmat(1,7) = - 1/6*A*ro*dCTxi*vr0^2; %KT*dCTxi;
Tmat(1,8) = - 1/6*A*ro*dCTxi*vr0^2;
Tmat(1,9) = - 1/6*A*ro*dCTxi*vr0^2;
Tmat(1,16)= - 1/2*A*ro*(dCTv*vr0^2 + ct0*2*vr0) ;%KT*dCTv;
Tmat(1,18)= - 1/2*A*ro*(-h*dCTv*vr0^2 - h*ct0*2*vr0) ;%KT*dCTv*h;

Tmat(3,1) = 0;
Tmat(3,4) = h*1/6*A*ro*dCTbeta*vr0^2; %KT/3*dCTbeta;
Tmat(3,5) = h*1/6*A*ro*dCTbeta*vr0^2;
Tmat(3,6) = h*1/6*A*ro*dCTbeta*vr0^2;
Tmat(3,7) = h*1/6*A*ro*dCTxi*vr0^2; %KT*dCTxi;
Tmat(3,8) = h*1/6*A*ro*dCTxi*vr0^2;
```

```
Tmat(3,9) = h*1/6*A*ro*dCTxi*vr0^2;
Tmat(3,16)= h*1/2*A*ro*(dCTv*vr0^2 + ct0*2*vr0) ;%KT*dCTv;
Tmat(3,18)= h*1/2*A*ro*(-h*dCTv*vr0^2 -h*ct0*2*vr0) ;%KT*dCTv*h;


Tmat = MredInv*Tmat;
Amat(16:18, :) = Amat(16:18, :) + Tmat;

%-------------------------------------------------------
%B-matrix
%-------------------------------------------------------
%u=[betaRef1 2 3 Pref]
Bmat = zeros(18,4);

Bmat(4,1) = 5;
Bmat(5,2) = 5;
Bmat(6,3) = 5;

Bmat(2,4) = -1/(2*Hs*wt0); %dwx/dP

%-------------------------------------------------------
%V-matrix
%-------------------------------------------------------
% v= [vind1 vind2 vind3 wave_x wave_z wave_theta]
Vmat = zeros(18,6);

Vmat(10,1)= KVV*dCPv + KV2; %dxi/dv
Vmat(11,2)= KVV*dCPv + KV2;
Vmat(12,3)= KVV*dCPv + KV2;

Vmat(16:18,1) = MredInv * [-KVT; 0; h*KVT] / 3;
Vmat(16:18,2) = MredInv * [-KVT; 0; h*KVT] / 3;
Vmat(16:18,3) = MredInv * [-KVT; 0; h*KVT] / 3;
Vmat(16:18,4:6) = MredInv;

%-------------------------------------------------------
%C-matrix
%-------------------------------------------------------
Cmat=eye(18);
%-------------------------------------------------------
%D-matrix
%-------------------------------------------------------
Dmat=zeros(18,10);

%-------------------------------------------------------
%State space system
%-------------------------------------------------------
mpcsys2 = ss(Amat, [Bmat Vmat],Cmat ,Dmat);
```

Appendix B

Simulink Diagrams

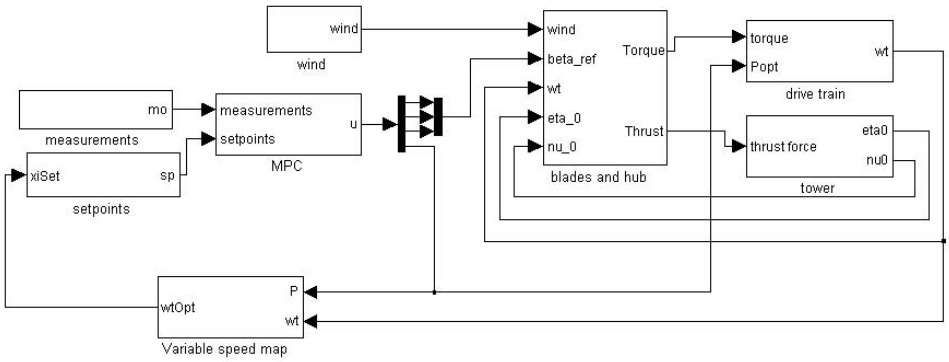

Figure B.1: Simulink diagram of the wind turbine simulator, with MPC controller

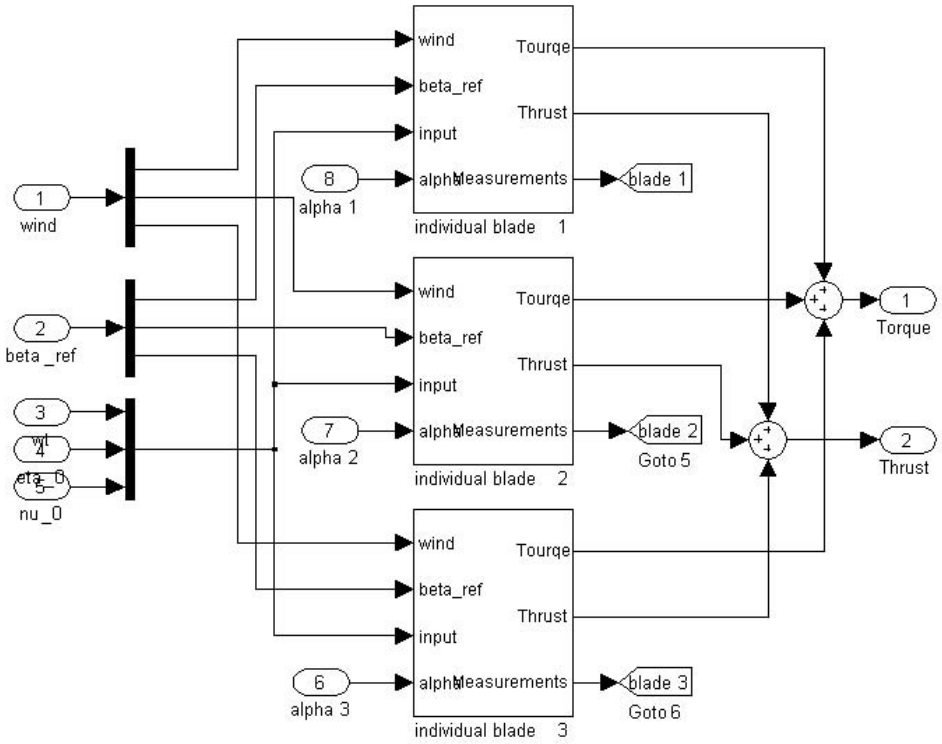

Figure B.2: Simulink diagram of the individual blades

Bibliography

Balchen, J. G., Andresen, T. & Foss, B. A. (2003), *Reguleringsteknikk*, Inst. for Tekn. Kybernetikk.

Beltran, B., Ahmed-Ali, T. & Benbouzid, M. E. H. (2008), 'Sliding mode power control of variable-speed wind energy conversion systems', *IEEE Transactions on Energy Conversion* **23**, 551–558.

Bianchi, F. D., Battista, H. D. & Mantz, R. J. (2007), *Wind Turbine Control Systems - Principles, Modeling and Gain Scheduling Design*, Advances in Industrial Control, Springer.

Bianchi, F. D., Mantz, R. J. & Christiansen, C. F. (2005), 'Gain scheduling control of variable-speed wind energy conversion systems using quasi-lpv models', *Control Engineering Practice* **13**, 247–255.

Bossanyi, E. A. (2003), 'Individual blade pitch control for load reduction', *Wind Energy* **6**, 119–126.

Bulder, B., Henderson, A., Huijsmans, R., Peeringa, J., Pierik, J., Snijders, E., van Hees, M., Wijnants, G. & Wolf, M. (2002), 'Floating offshore wind turbines for shallow waters'.

Butterfield, S., Musial, W., Jonkman, J. & Sclavounos, P. (2007), Engineering challenges for floating offshore wind turbines, National Renewable Energy Laboratory.

Chen, C.-T. (1999), *Linear Systems Theory and Design*, Oxford University Press.

Chincilla, M., Arnaltes, S. & Burgos, J. C. (2006), 'Control of a permanent-magnet generators applied to variable-speed wind energy systems connected to the grid', *IEEE Transactions on Energy Conversion* **21**(1), 130–135.
URL: *http://ieeexplore.ieee.org/stamp/stamp.jsp?arnumber=1597329&isnumber=33594*

Doyle, J. C. (1978), 'Guaranteed margins for lqg regulators', *IEEE Transactions on Automatic Control* **AC-23**, 756–757.

DWIA (2003), 'Danish wind industry association - wind energy reference manual'.
URL: *http://www.windpower.org/en/stat/unitsw.htm#roughness*

Eggleston, D. M. & Stoddard, F. S. (1987), *Wind Turbine Engineering Design*, Van Nostrand Reinhold Company.

EWEA (2008), 'Wind energy scenarios up to 2030'.
URL: *http://www.ewea.org/fileadmin/ewea_documents/documents/publications/reports/purepower.pdf*

Fossen, T. I. (2002), *Marine Control Systems*, Marine Cybernetics.

Fossen, T. I. (2009), *Modelling and Control of Marine Vessels*, Marine Cybernetics.

Fuglseth, T. P. & Undeland, T. (2007), Modeling of floating wind turbine platforms for controller design. Nordic Wind Power Conference.

Hansen, A. D. & Michalke, G. (2008), 'Modeling and control of variable speed multi-pole permanent magnet synchronous generator wind turbine', *Wind Energy* **11**, 537–554.

Hau, E. (2006), *Wind Turbines - Fundamentals, Technologies, Application, Economics*, 2 edn, Springer.

Jonkman, J., Butterfield, S., Musial, W. & Scott, G. (2009), Definition of a 5-mw reference wind turbine for offshore sustem developement, Technical report, NREL.
URL: *http://www.nrel.gov/docs/fy09osti/38060.pdf*

Kallesøe, B. S. (2006), 'A low-order model for analysing effects of blade fatigue load control', *Wind Energy* .
URL: *http://www3.interscience.wiley.com/cgi-bin/fulltext/112533071/PDFSTART*

Knauer, A., Hanson, T. D. & Skaare, B. (2006), Offshore wind turbine loads in deep-water environment, *in* 'EVEC 2006'.

Larsen, A. J. & Mogensen, T. S. (2006), Individuel pitchregulering af vindmølle, Master's thesis, Tech. Uni of Denmark.

Larsen, T. J. & Hanson, T. D. (2007), 'A method to avoid negative damped low frequent tower vibrations for a floating, pitch controlled wind turbine', *The Science of Making Torque from Wind, Journal of Physics* **75**.

Lemming, J. K., Morthorst, P. E. & Clausen, N.-E. (2007), 'Offshore wind power - experiences, potential and key issues for deployment'. Risø National Laboratory.
URL: *http://www.iea.org/textbase/work/2007/offshore/background.pdf*

Maciejowski, J. (2002), *Predictive Control with Constraints*, Prentice-Hall.

Manwell, J., McGowan, J. & Rogers, A. L. (2002), *Wind Energy Explained - Theory, Design and Application*, Wiley.

MarinTek (2007), Floating wind turbine analysis - survey of analysis tools. Written for Sintef Energiforskning. Not published.

Munteanu, I., Bratcu, A. I., Cutululis, N.-A. & Ceanga, E. (2008), *Optimal Control of Wind Energy Systems*, Springer.

Nichita, C., Luca, D., Dakyo, B. & Ceanga, E. (2002), 'Large band simulation of the wind speed for real time wind turbine simulators', *IEEE Transactions on Energy Conversion* **17**(4), 523–530.
URL: *http://ieeexplore.ieee.org/stamp/stamp.jsp?tp=&arnumber=1159204&isnumber=25975*

Nielsen, F. G., Hansen, T. D. & Skaare, B. (2006), 'Integrated dynamic analysis of floating offshore wind turbines', *Proceedings to the EWEC 2006* .

Nielsen, F. G., Skaare, B., Tande, J. O. G., Norheim, I. & Uhlen, K. (2008), 'Method for damping tower vibrations in a wind turbine installation'.

NVE (2009), 'Vindkraft - produksjonsstatistikk - 2008', Report.

Quirante, J. J. G. (2007), Control of wind tiurbines for power regulation and load reduction, Master's thesis, Tech. Uni. of Denmark.

Safonov, M. G. & Athans, M. (1977), 'Gain and phase margin for multiloop lqg regulators', *IEEE Transactions on Automatic Control* **AC-22**, 173–179.

Selvam, K. (2007), Individual pitch control for large scale wind turbines - multi-variable control approach, Master's thesis, TU Delft - Delft Centre for Systems and Control.

SintefEnergyResearch (2005), Flytende offshore vindkraftverk - utvikling av dynamisk simuleringsmodell. Arbeidsnotat AN 05.12.55.

Skaare, B. (2009), 'Method for the damping of tower oscillations in wind power installations'.

Skaare, B., Hanson, T. D. & Nielsen, F. G. (2007), 'Importance of control strategies on fatigue life of floating wind turbines', *Procedings of the26th International Conference on Offshore Mechanics and Arctic Engineering* .

Skogestad, S. & Postletwaite, I. (2005), *Multivariable Feedback Control*, John Wiley & Sons, Ltd.

Slotine, J.-J. & Li, W. (1991), *Applied Nonliear Control*, Prentice-Hall.

Spong, M. W., Hutchinson, S. & Vidyasagar, M. (2006), *Robot Modeling and Control*, Wiley.

StatoilHydro (2009), 'Hywind fact sheet'.

St.meld nr.34 (2006-2007). Stortinggsmelding nr. 34 - Norks Klimapolitikk.
URL: *http://naring.enova.no/sitepageview.aspx?sitePageID=1138*

sway.no (2008), webpage.
URL: *www.sway.no*

van den Boom, T. J. J. & Backx, T. C. P. M. (2007), *Lecture Notes on Model Predictive Control*, TU Delft - Faculteit 3mE.

Wayman, E. N., Sclavounos, P. D., Butterfield, S., Jonkman, J. & Musial, W. (2006), Coupled dynamic modeling of floating wind turbine systems, National Renewable Energy Laboratory.
URL: *http://www.nrel.gov/wind/pdfs/39481.pdf*

Weisstein, E. W. B. F. F. M.-A. W. W. R. h. (n.d.), '"beta function." from mathworld–a wolfram web resource. http://mathworld.wolfram.com/betafunction.html'.
URL: *http://mathworld.wolfram.com/BetaFunction.html*

Windsea.no (2008), webpage.
URL: *http://www.windsea.no/*